

Alma Mater Studiorum – University of Bologna

School of Engineering and Architecture

Department of Electrical, Electronic and Information Engineering (DEI)

Master Course in
Electrical Energy Engineering

Thesis in:
APPLIED MEASUREMENTS FOR POWER SYSTEMS

**Metrological characterisation of Low Power
Voltage Transformers by using impulse
response analysis**

Student:

Saeid Homeili

Supervisor:

Prof. Lorenzo Peretto

Academic year: 2019/2020

JULY 2020

Acknowledgment:

To my beloved wife and son which has always supported me...

To my bleeding home Iran which will be in my heart forever...

To Italy which gave me this golden opportunity through the scholarship program of the Italian Ministry of Education Affairs...

*I would like to express my special thanks of gratitude to my supervisor Prof. **Lorenzo Peretto** who helped me to do this thesis and to obtain new knowledge and special thanks to my best friend Dr. Abass Ghaderi who help me to find answers to do this thesis.*

INDEX

INTRODUCTION

CHAPTER 1

1	STATE OF THE ART	9
1.1	The necessity of voltage and current measurement	9
1.2	Modeling and identifying of LPITs	10
1.3	Impulse response application background	12

CHAPTER 2

2	LITERATURE REVIEW	15
2.1	Voltage and current measurement	15
2.2	conventional current transformer (CT)	15
2.3	Main features of current transformers.....	16
2.4	Voltage transformer (V.T.)	17
2.5	Capacitor voltage transformer (C.V.T.).....	18
2.6	The new generation of LPITs	22
2.7	Technical consideration	23
2.8	Accuracy in LPVT and LPCT.....	24
2.9	New generation of medium current transformer (LPCT)	25
2.10	The new generation of medium voltage transformer (LPVT)	27
2.10.1	Passive LPVT	27
2.10.2	Active LPVT	29
2.11	LPVT (smart terminals)	30
2.12	Insulations consideration	31
2.13	Dielectric permittivity in LPITs.....	31
2.13.1	The dielectric of a capacitor	33
2.13.2	Specification factors in a capacitor.....	34
2.13.3	Dissipation factor and loss of tangent definitions	35
2.14	Frequency dependency to the permittivity.....	35

CHAPTER 3

3	PROCEDURE	40
3.1	The dynamic model of LPVT	41
3.2	Unit impulse function	43
3.2.1	Sampling property	43
3.3	Study of impulse response system identification.....	44
3.4	Definition of transfer function using impulse response.....	46

3.4.1	Convolution integral	47
3.4.2	FFT and IFFT concept	50
3.5	Sinc function as an impulse signal	51
3.6	Sinc function properties	52
3.7	Power quality frequency range	56
3.8	Design the sinc signal	57
3.8.1	DTFT	57
3.8.2	Bandlimited pulse (window pulse)	58
3.8.3	Sinc calculation	61
3.9	Measured parameters and tests	66
3.9.1	Sinc response test	67
3.9.2	Sweep frequency response test	68
3.10	The transfer function of LPVT	68
 CHAPTER 4		
4	EXPERIMENTAL TEST	71
4.1	Setup test	71
4.1.1	Arbitrary Waveform	73
4.1.2	Data Acquisition Chain	75
4.2	Measurement setup	77
4.3	Approval and validation tests	79
4.3.1	Sinc response test in different voltages validation	79
4.3.2	Harmonic tests validation	80
 CHAPTER 5		
5	RESULTS	82
5.1	Results of a new method of sinc response	82
5.1.1	SR test results	82
5.1.2	Sweep frequency test results and comparison	83
5.2	$h(t)$ transfer function	84
5.3	Approving $h(t)$ accuracy	86
5.3.1	Result test under different voltage and frequencies	86
5.4	Results of harmonics test and validation of $h(t)$	88
5.4.1	Sinusoidal harmonic results	89
5.5	Validation of $h(t)$	91
6	CONCLUSION	94
	REFERENCES	96

Introduction

The evolution of smart grids and the broad application of renewables and medium voltage (MV) industries have created a need for the extensive use of current and voltage measurements for the proper management of power networks. Electrical power grids will require real-time capable control and monitoring systems to ensure stability under increasingly complex and challenging conditions. The generation of analog measurement and control systems in power substations are approaching the end of their useful lifespan. More often their replacement is based on digital substation automation solutions and the use of new technologies to perform more efficiently. In distribution, measurements and control of the power network, require the use of advanced, low-power sensing technologies instead of traditional solutions using iron-core instrument transformers, due to their physical limitations and other reasons. Moreover, Instrument Transformers are experiencing special attention by utilities and private customers for different important reasons.

A generally accepted propose is the installation of a low-power current transformer (LPCT) (current sensor) and a low-power voltage transformer (LPVT) (voltage sensor) due to accurate operation, high bandwidth, small size and compatibility with computer network in digital substation automation. The application of an LPCT is not so demanding from an electrical field point of view and different technologies can even be used. Nevertheless, the application of an LPVT needs to access the MV point, which is a challenging task to separable connectors due to the high level of electric field strength in the under-voltage area.

The requirements of LPVTs are described in the existing standard IEC 60044-7, released in 1999, and a new set of standards for the IEC 61869 standard family to cover the latest needs and requirements for both active and passive LPVTs are introduced in recent years. These standards describe a set of tests. LPVTs have some test requirements that apply to each particular product. These requirements are not always aligned, as they demand different tests, different test values, or different acceptance criteria, which depend on other specific requirements agreed upon between the manufacturer and purchaser. On the other hand, the achieved results of these tests can not cover all the needs to characterize LPVT, specifically covering accuracy requirements or give valuable identity which capable to introduce LPVT behavior in different conditions. Also, many of these tests are time-consuming and are not always aligned.

Therefore, this thesis presents a new approach in dealing with this issue and proposes determining the impulse response of LPVT, purposing to find transfer function ($h(t)$) which contains most electrical characteristics of LPVTs as a dynamic system. To characterize any dynamic system impulse Response is a well-known approach in literature to identify the behavior of LPVTs, This thesis also suggests using sinc function as an impulse signal to achieve response in determining frequency band. Additionally, the proposed approach has been approved and validated by extensive, practical testing of passive LPVT in design experimental setup in laboratory and computer simulations, the results of these tests passed by comparing results with simulation and standard. Finally, the recommended method and test approaches and criteria can be proposed improvement of future IEC 61896-11 standards.

The thesis is structured as follows:

1. In Chapter One, the necessity of voltage and current is expressed. Importance of modeling and types of modeling for system identification are mentioned, some application of using impulse response in some different surveys are introduced.
2. In Chapter Two some features and definitions about the conventional CT, PT, CVT, and in the following LPCT and passive and active LPVT are explained, also structure of capacitor LPVT and relevant relation and impact of dielectric permittivity on frequency response in a capacitor is mentioned.
3. In Chapter Three, it is tried to define the LPVT model. A proper dynamic system by using control theory and signal system concept is expressed. Application of impulse response in identifying and characterization in some articles and surveys which have been studied up to now are explained. In the following the new method using sinc signal to apply as an impulse signal and also an analytical approach to design sinc signal in power quality frequency domain is expressed. Moreover, all procedure tests which are designed to approve this method and tests for validation of the sinc response and validation of LPVT transfer function $h(t)$ are explained at the end of this chapter.
4. In chapter Four experimental setup tests and all utilize apparatus and components and also the software is explained, relevant schematics and setup tests are depicted. All processes of tests and simulation due to the approval and validation of the results are explained.
5. In chapter Five the result of sinc response and sweep frequency response are explained and analyzed. Moreover, to approve the accuracy of the purpose method the result of sinc response to different voltages in different frequencies is compared with simulation results. Test results by the different sinusoidal signal which are contaminated with different harmonics are shown and recorded and admitted by comparing with experimental test. In

the end, the simulation results of accuracy of LPVT transfer function $h(t)$ are validated by comparing simulation results with standard value for sinusoidal harmonics, all results are depicted via relevant diagrams, charts, and tables.

CHAPTER 1

STATE OF THE ART

1 STATE OF THE ART

In modern society, in this age of advanced technology, using a complex chain of electrical and electronic systems should inevitably have one hundred percent integrity. A failure is considered unacceptable from customers' perspective, and any implications or consequences due to failure have been significant in most of all aspects of modern life. Therefore, in various engineering applications that involved electrical transmission and distribution systems, for instance: industries, smart grid, distribution generation, and power quality, etc. There are committed to seek and develop advanced technology which guarantees better performance and efficiency for the normal operation of various interconnected electrical networks and systems.

One of the major system that mentioned is the system in which efforts to measure accurate and real-time electrical parameters. Protection relays, power meters, and control units in up-to-date switchgear are built with digital technology. The modern secondary equipment does not need the high power output of the instrument transformers (ITs) as this was necessary for electromechanical relays. As a consequence, the requirements for (ITs) is changed. Requests for universal use of (ITs) for measurement, protection, and even metering applications and the reduction of the overall costs of switchgear are common. Further requirements for modern (ITs) besides reliability and safety are easy handling, the reduction of the expenditure of work during planning and installation, and short lead times.[1] By using established and highly proven components such as iron cores, capacitors, resistors, and quadrat pole shunt it is possible to produce sensors which are fulfilling all the requirements. Compared with traditional (ITs), low power (ITs) have less overall costs, lower weight, and are immune to electromagnetic interference in the substation. One low power (IT) can be used for metering and protection purposes. For that reason, the number of different types for all applications can be dramatically reduced in a wide range of primary current.

Nowadays digital instruments, apparatuses, and relays with inputs for low power (ITs) are available from several relay manufacturers. By using such relays together with the wide measuring range of low power (ITs) users get a system with high reliability, functionality, and flexibility. Considering short review of typical current and voltage sensors gives clear aspects of (ITs) sensors. [2]

1.1 The necessity of voltage and current measurement

CT & PT are called the instrument transformer, because those are used to assist the measuring instruments for the measurement of electrical parameters like current, voltage, frequency,

power factor, active power(MW), reactive power(MVAR), etc. of high voltage system. The high current & high voltage of a high voltage system cannot be directly fed to a measuring instrument for measurement purposes and protection chains, as the instrument will be damaged or burnt. So the high current/voltage is reduced to a reasonably small value i.e. 5 amp, or 1 amp, in case of current transformer and 110 volts, in case of a voltage transformer. These are called the secondary current or voltage which is directly proportional to the primary current or voltage. This secondary current or voltage is conveniently fed to the measuring instruments and relays, which in turn can measure the primary parameters with a suitable scale. Moreover, it enhances safety for the personnel at the low voltage control and protection side and makes it possible for standardization of instruments, relays, power quality meters, load flow calculation, and PMU system. And also, attain other quantities that are involved with control, estimate, planning, maintenance, and operation on generation in power plants, transmission networks, and distribution systems. Conventional steady-state analysis of power networks relies on the so-called bus/branch model. Accordingly, the active and reactive power flows through switches and circuit breakers are treated as state variables along with the complex voltage at the network nodes, and also the case of real-time modeling, where the current trend is towards the representation of parts of the power network at the bus-section. The search of the correct network topology requires the consideration of voltage and current measurements using (LPITs) in nodes and through the branches respectively. [3]

1.2 Modeling and identifying of LPITs

For better reorganization of feature and identify the behavior of (ITs), studying on a clear model of (ITs) as a system can be the main way to analysis of behavior (IT's) functionality. Modeling is an essential tool for engineers to assess the functions of apparatus and components as dynamic systems. [4]

In control system engineering, system identification methods are used to get appropriate models for the design of prediction algorithms, or simulation. Also in signal processing applications, models obtained by system identification are used for (spectral analysis, fault detection, pattern recognition, adaptive filtering, linear prediction), and other purposes. In recent times, system identification techniques have delivered powerful methods and tools for data-based system modeling. While the theory for identification of linear systems has become very mature, the challenges for the field are in modeling and developing more complex dynamical systems (nonlinear, distributed, hybrid, large scale), and in task-oriented issues

(identification for control, diagnosis, etc.). They also have wide applications in non-technical fields such as biology, environmental sciences, and econometrics to develop models for increasing scientific knowledge on the identified object, or prediction and control. [5] In this thesis, it is purposed the develop a dynamic model of (ITs) that has a weighting function that coincides with an estimated sequence.

Dynamic systems are described by differential equations. The solution of the differential equation will be able to see the impact of the input, it shows how the variables of the system depend on the independent variable. Through modeling, we have converted our suspension into a system, with input, output, states, and parameters. [6] System identification deals with the problem of constructing the mathematical model of a dynamic system based on a given set of experimental data. To perform a theoretical analysis of the identification methods, it is necessary to introduce assumptions on the data. As it is not necessary to know the system, we will use the system concept only for investigating how different identification methods behave under different circumstances such as the behavior of system interacting to supply impulse signal or step signal.

The purpose of a model is to describe how the various variables of the system relate to each other. The relationship among these variables is called a model of the system. Modeling the system of interest is considered useful in many areas of science as an aid to properly describe the system's behavior. A good model must reflect all properties of such an unknown system. Several kinds of models can be classified as mental models that do not involve a mathematical formula, graphical models that are also suitable for certain systems using numerical tables and/or plots. Mathematical models which describe how the variables relate to each other in terms of mathematical expressions such as differential and difference equations. The mathematical models are useful in practice because they describe the system's behavior by mathematical expressions, which are simple to examine and analyze. [6]

In many cases, while dealing with problems related to system identification we deal with parametric models, such models are characterized by a parameter vector, which we denote by θ . The corresponding model will be denoted $M(\theta)$. When θ is varied over a set of feasible values we obtain a model structure.

Sometimes, we use non-parametric models such as a model that is described by a curve, function, or table. An impulse response is an example of these models which we will study later in detail in this thesis.

The property by which the resulting models are in forms of curves or functions so that the identification method is known to be a non-parametric method. One of the nonparametric methods which are used is the impulse response. The impulse response of a system is its output when presented with a brief signal, an impulse. While an impulse is a difficult concept to imagine, it represents the limit case of a pulse made infinitely short in time while maintaining its area or integral (thus giving an infinitely high peak). [7]

1.3 Impulse response application background

In literature, there are many studies on the implementation of an impulse response. There can be addressed varied applications and researches which are commented in the following:

1-Test and approve of protection capability oil insulation breakdown in transformer and other apparatus and capability of withstanding extra-high voltages to protect the measurement devices during the high voltage test(partial discharge detection experiments, breakdown, etc.)[8]

2- Frequency response analysis (FRA) is a regular method to detect winding faults in the transformer. According to the kind of excitation source it can be used impulse frequency response analysis (IFRA) and sweep frequency response analysis (SFRA) However, it has been discovered that the test result of IFRA can be heavily influenced by the repetition frequency of input impulse. Besides, the frequency resolution of the test result also needs to be considered. Winding deformations are major faults that occur in the power transformer and Frequency response can be plot as a trend with resonances at several different frequencies, these resonances are produced by the inductance and capacitance of the network. Based on the information of the response trend, especially the frequencies of resonances, small deformation of transformer winding can be detected by imposing the impulse signal to the transformer. The impulse signal has higher amplitude and frequency band than the sinusoidal signal, which means that the signal to noise ratio (SNR) is better and the frequency response curve can reach to frequency higher more than 1MHz, providing more information about the characteristic of the transformer.[9]Moreover, impulse frequency response analysis (IFRA) is feasible for online condition monitoring of power transformer winding deformation and can increase the

frequency range of analysis. At present, the Frequency response curves of off-line IFRA methods are mostly solved by Fast Fourier Transform (FFT). [10]

3- by using the method based on Wiener filtering and measurement of the transformer response in the frequency domain using a low-frequency network analyzer it can possible to present a method for Finite-Impulse-Response (FIR) modeling of voltage instrument transformers.[11]

4-by using impulse response which is applying to Instrument Voltage Transformers (VT), it can be capable of analyzing critical behavior such as inaccuracy and ratio error in VT.[12] So, output signals may result in terms of overvoltage able to provoke dangerous dielectric solicitations when subjected to impulse voltages. Furthermore, the accuracy of VT (defined by IEC Standards) only at power frequency doesn't consider fast impulse response. Under these conditions, the VT may introduce errors in voltage measurements and the transmitted signals may create overvoltage in correspondence of the secondary circuit and by nominal withstand.[13] Additionally, the transformer ratio (peak values) under impulse condition was found to be normally lower (2-3 times) than the nominal value and this error may have negative Consequences also in terms of power quality. [14]

5-Their has been used as finite impulse response (FIR) model for prediction of the process outputs in many studies. In contrast to state-space parameterizations, the FIR model is in a form that can easily be applied in robust predictive control, i.e.[15]

In many science branches and survey phenomenon using an analysis of impulse response is a known tool and also an efficient way to reach an acceptable result. It can be mentioned to impulse response analysis to study and measure parameters of state variables in acoustic spaces or transducers or widespread use in communication science[16],[17].

Just as utilization of impulse response analysis is the so-called method for finding the many answers, and also it is a progress technique to achieve the right behavior of systems in various electrical apparatuses and relevant functions.

This thesis is going to study using impulse response to find out the behavior characteristics and responses of LPVTs to impulse signals. Hence, to a better understanding of characteristics and different current and voltage transformers, it is tried to explain some features and brief mention to introduce conventional CTs, PTs, CVT. Afterward, new generations of LPCTs, LPVTs will be considered.

CHAPTER 2

LITERATURE REVIEW

2 LITERATURE REVIEW

Interconnected power systems are usually subdivided into different control and security areas. The transmission system operator is the responsible entity for the security of a single control area. Generally, voltage and frequency control and the security level assessment are the main tasks to keep the system in the normal state.

Voltage control of power systems is mainly provided by the generating units. The terminal voltage of generating units is controlled and maintained within specific limits utilizing the automatic voltage regulator (AVR). The frequency of an electric system depends on the active power balance. To control the frequency, the active power balance must be restored. The typical measurement of voltage in terminals and buses and current in branches are utilized to power balance, voltage control and have reliable security of electrical system operating at different voltage levels.

2.1 Voltage and current measurements

Current and voltage transformers (CT/PT) are used in High Voltage (HV) and Medium-voltage (MV) Installations to give an of electrical current to protection relays and units and metering equipment and they are designed to value to provide a current and voltage in its secondary proportional to the current flowing in its primary. CTs are connected in series and protection devices and metering equipment is connected to the secondary of the CT in a series association. And PTs are connected in parallel.

2.2 conventional current transformer (CT)

To better understand CT characteristics and functionality some important features and operational parameters are explained Current and voltage transformers are generally designed in the following standards:

IEC 60044-1 “current transformers”, IEC 60044-2 “inductive voltage transformers” ANSI/IEEE-standard, all other relevant worldwide standards.

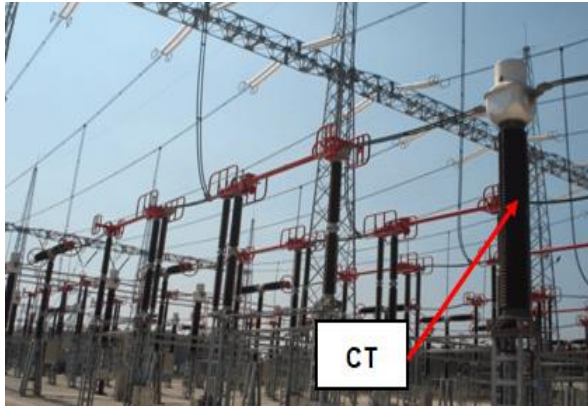


Fig.2-1 Current transformer in an AIS substation

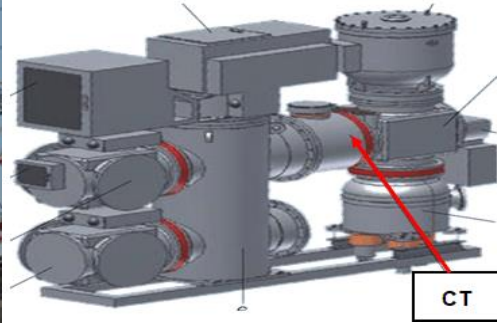


Fig. 2-2 Current transformer in a GIS substation

2.3 Main features of current transformers

There are several features and characteristics introduced by factories according to the application and technical points of view. In this part, the main, well-known and most practical is presented

- **Rated primary current**

The value of the primary current which appears in the designation of the transformer and on which the performance of the current transformer is based.

- **Rated secondary current**

The value of secondary current which appears in the designation of the transformer and on which the performance of the current transformer is based. Typical values of secondary currents are 1 A or 5 A. In the case of transformer differential protection, secondary currents of $1/\sqrt{3}$ A and $5/\sqrt{3}$ A is also specified.

- **Rated burden**

The apparent power of the secondary circuit in Volt-amperes expressed at the rated secondary current and a specific power factor (0.8 for almost all standards)

- **Accuracy class**

In the case of metering CT s, accuracy class is typical, 0.2, 0.5, 1, or 3. This means that the errors have to be within the limits specified in the standards for that particular accuracy class. The metering CT has to be accurate from 5% to 20% of the rated primary current, at 25%, and 100% of the rated burden at the specified power factor. In the case of protection CT s, the CT s should pass both the ratio and phase errors at the specified accuracy class, usually 5P or 10P, as well as a composite error at the accuracy limit factor of the CT.

- **Current ratio error**

The error with a transformer introduces into the measurement of a current and which arises from the fact that the actual transformation ratio is not equal to the rated transformer ratio. The current error expressed in percentage is given by the formula:

$$\text{Current error in \%} = (K_a (I_s - I_p)) * 100 / I_p \quad (2.1)$$

Where (K_a) is rated transformation ratio, (I_p) is actual primary current, (I_s) is actual secondary current when I_p is flowing under the conditions of measurement.

- **Knee point voltage**

That point on the magnetizing curve (Fig.2-3) where an increase of 10% in the flux density (voltage) causes an increase of 50% in the magnetizing force (current). The 'Knee Point Voltage' (V_{kp}) is defined as the secondary voltage at which an increase of 10% produces an increase in magnetizing current of 50%. It is the secondary voltage above which the CT is near magnetic saturation.

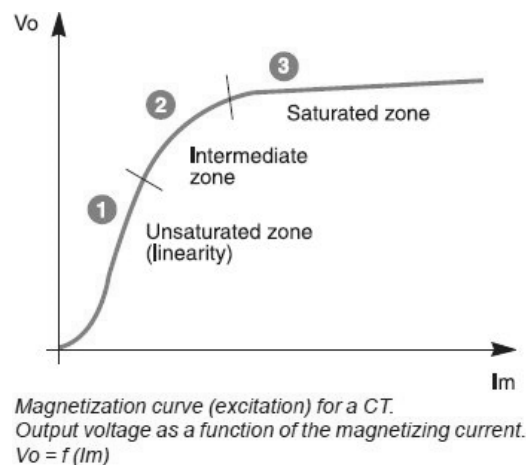


Fig. 2-3

2.4 Voltage transformer (V.T.)

The potential transformer may be defined as an instrument transformer used for the transformation of voltage from a higher value to a lower value. This transformer step down the voltage to a safe limit value which can be easily measured by the ordinary low voltage instrument like a voltmeter, wattmeter and watt-hour meters, etc.

- **Construction of potential transformer**

The potential transformer is made with high-quality core operating at low flux density so that the magnetizing current is small. The terminal of the transformer should be designed so that the variation of the voltage ratio with load is minimum and the phase shift between the input and output voltage is also minimum.

The primary winding has a large number of turns, and the secondary winding has a much small number of turns. For reducing the leakage reactance, the co-axial winding is used in the potential transformer. The insulation cost is also reduced by dividing the primary winding into the sections which reduced the insulation between the layers.

- **Connection of potential transformer**

The potential transformer is connected in parallel with the circuit (Fig.2-4). The primary windings of the potential transformer are directly connected to the power circuit whose voltage is to be measured. The secondary terminals of the potential transformer are connected to the measuring instrument like the voltmeter, wattmeter, etc.

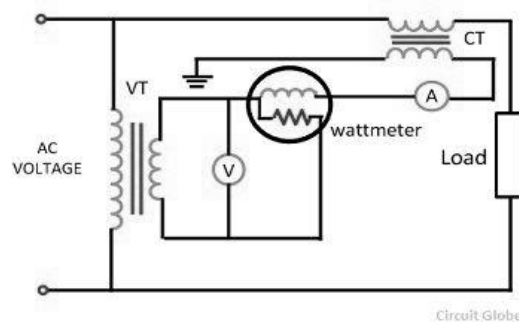


Fig. 2-4

The secondary windings of the potential transformer are magnetically coupled through the magnetic circuit of the primary windings.

2.5 Capacitor voltage transformer (C.V.T.)

The potential transformer is mainly classified into two types, i.e., the conventional wound types (electromagnetic types) and the capacitor voltage potential transformers. In this thesis, we focus on capacitor voltage. Conventional wound type transformer is very expensive because of the requirement of the insulations. Capacitor potential transformer is a combination of capacitor potential divider and a magnetic potential transformer of a relatively small ratio. [18],[19],[20].

A capacitive voltage transformer (CVT) is widely used in high-voltage (HV) and extra-high voltage (EHV) and medium voltage systems instead of a traditional voltage transformer (VT). (Fig.2-5) is illustrated a CVT's structure can be mainly divided into a capacitive divider and an electromagnetic unit. A capacitive divider is comprised of an insulating cylinder and a series capacitors inside of it. An electromagnetic unit is comprised of a compensation reactor, a step-down transformer, and a damper. A capacitive divider can first lower the system voltage as an input for an electromagnetic unit. By isolation and reduction of the step-down transformer, the low voltage signals can be used for protection and measurement. Compared with a VT, a CVT has the advantages of smaller size, lower cost, and refrain from Ferro resonance. However, the structure of a CVT is more complicated than a traditional VT which has more measurement accuracy influential parameters, therefore a CVT has more significant measurement error and a higher probability of insulation faults. The circuit diagram of the capacitor potential transformer is shown in the (Fig.2-6). The stack of high voltage he capacitor from the potential divider, the capacitor of two sections becomes C_1 and C_2 .

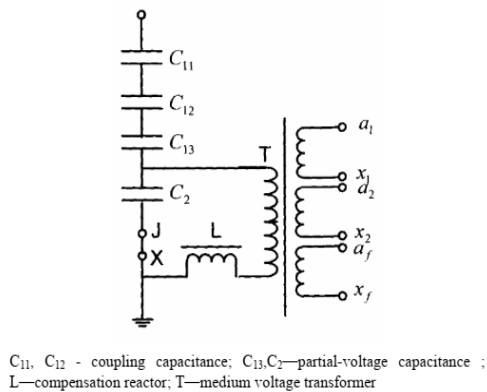
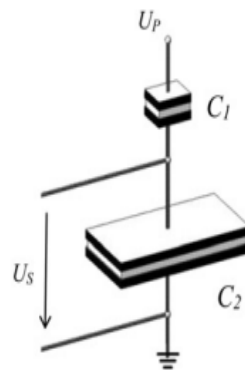


Fig. 2-5



$$u_S(t) = \frac{C_1}{C_1 + C_2} u_P(t)$$

Fig. 2-6

Both potential dividers and the intermediate transformer have the ratio and insulation requirements which are suitable for economical construction. The intermediate transformer must be of very small ratio error, and phase angle gives the satisfactory performance of the complete unit. The secondary terminal voltage is given by the formula shown below. [21]

- CVT model

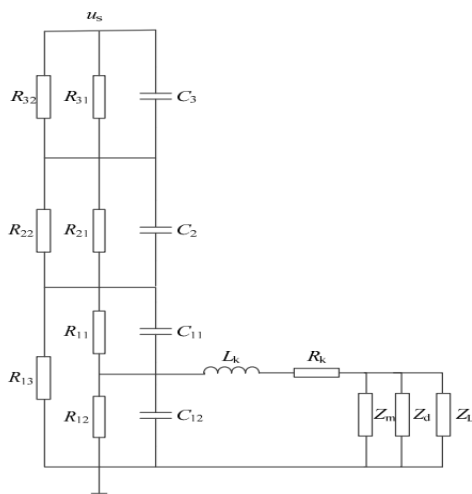


Fig. 2-7

In (Fig.2-7) capacitors are named as the first, second, and third capacitor from bottom to the top in the voltage divider respectively. C_{11} , C_{12} , C_2 , and C_3 are the equivalent capacitance of each segment, where C_{11} , C_2 , and C_3 belong to the high-voltage capacitor, and C_{12} belongs to the low-voltage capacitor. The main factors influencing equivalent capacitance are temperature and dielectric breakdown. Since a CVT capacitor has a negative temperature coefficient, the equivalent capacitance will decrease when the temperature increases. The dielectric breakdown will cause a short circuit in series capacitors, which means equivalent capacitance will increase. R_{11} , R_{12} , R_{21} , and R_{31} are the insulation resistances of each segment. The increase in the dielectric loss factor represents a decrease in insulating resistance. The main factors influencing insulation resistance are temperature and moisture in the insulation. When the temperature increases, the dielectric loss of the capacitor will first decrease and then increase. Therefore, the corresponding insulation resistance will first increase and then decrease. Moisture in the insulation will result in a larger dielectric loss, which means the insulation resistance will decrease. R_{13} , R_{22} , and R_{32} are the surface equivalent resistances. The increase in leakage current represents a decrease in surface resistance. The main factors influencing the surface resistance is environmental contamination and humidity. When contamination and humidity in the atmosphere increases, the surface leakage current of a capacitive divider will increase, which represents the decrease in surface resistance. The electromagnetic unit, L_k , is the sum of compensation reactor reactance and leakage reactance of the transformer, which can be used to resonate with equivalent capacitance of the voltage divider c_0 , $L_k = 1 / \omega^2 c_0$. R_k is the sum of tuning reactor resistance and short

circuit resistance of the transformer; Z_m is the excitation impedance of the transformer; Z_d and Z_L are the impedance of the damper and load which are recalculated to the primary side of the step-down transformer. $\tan\delta$ is the dielectric loss factor(2.2) which can be used to characterize the real power loss of insulating material. [21]

$$\tan\delta = 1/\omega RC \quad (2.2)$$

In an ideal potential transformer, the primary and the secondary voltage is exactly proportional to the primary voltage and exactly in phase opposition. But this cannot be achieved practically due to the primary and secondary voltage drops. Thus, both the primary and secondary voltage is introduced in the system.

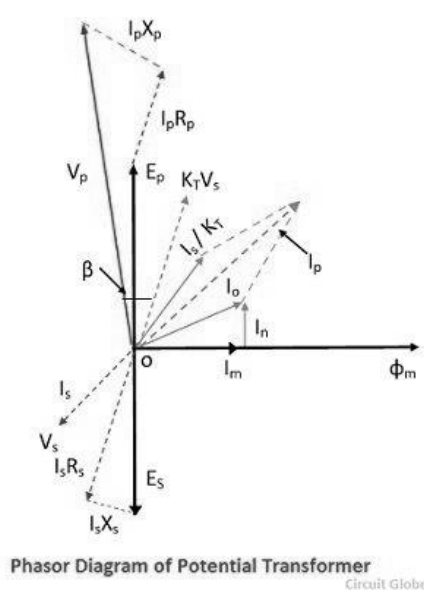
- **The burden of a potential transformer**

The burden is the total external volt-amp load on the secondary at the rated secondary voltage. The rated burden of a PT is a VA burden which must not be exceeded if the transformer is to operate with its rated accuracy. The rated burden is indicated on the nameplate.

The limiting or maximum burden is the greatest VA load at which the potential transformer will operate continuously without overheating its windings beyond the permissible limits. This burden is several times greater than the rated burden. [22]

- **Phasor diagram of a potential transformer**

The phasor diagram of the potential transformer is shown in the (Fig.2-8).



- Where, I_s – secondary current
- E_s – secondary induced emf
- V_s – secondary terminal voltage
- R_s – secondary winding resistance
- X_s – secondary winding reactance
- I_p – Primary current
- E_p – primary induced emf
- V_p – primary terminal voltage
- R_p – primary winding resistance
- X_p – primary winding reactance
- K_t – turn ratio
- I_o – excitation current
- I_m – magnetizing component of I_o
- I_w – core loss component of I_o
- β – phase angle error

Fig. 2-8

The main flux is taken as a reference. In instrument transformer, the primary current is the vector sum of the excitation current I_0 and the current equal to the reversal secondary current I_s multiplied by the ratio of $1/k_t$. The V_p is the voltage applied to the primary terminal of the potential transformer. [23],[24]

The accuracy class is guaranteed if the voltage is between 80 and 120% of the rated primary voltage and for any load between 25 and 100% of the rated accuracy power with an inductive power factor of 0.8.[25],[26]

TABLE I. the accuracy class generally used by the corresponding application.

Application	Accuracy class
Not used in industry	0.1
Precision metering	0.2
Usual metering	0.5
Statistical metering and/or measurement	1
Measurement not requiring high accuracy	3

2.6 The new generation of LPITs

The use of instrument transformers is mandatory for protection or measuring in Medium Voltage applications. Technological progress has led to many developments in the field of measuring. In Medium Voltage applications, the consequence comes into using more and more LPITs associated with digital relays. Relays are easily fitted with LPCTs, ensuring a high consistency of the devices building the protection chain. The LPITs have an output signal with a limited maximum power around 1 volt-ampere, hence a few volts or mil-amperes, that are suitable to direct connect to an acquisition system, avoiding the use of signal adapters that complicate the measurement setup and may decrease its overall accuracy. Another peculiarity of the LPITs is the dimension, which is more compact and reduced compared to legacy inductive ones. This feature of the LPITs is particularly appreciated in a Smart Grid environment where the distributed energy resources, mainly constituting renewable sources, require that the measurement instruments are installed in an application where the space for them is limited and not guaranteed. [27]

- **VT versus LPVT and CT versus LPCT**

Table II summarizes the pros and cons of conventional voltage transformers (VTs) and current transformers (CTs) compared to the new low-power voltage transformers (LPVT) and low-power current transformers (LPCT).[28]

TABLE II summarizes the pros and cons of (VTs) and (CTs) compared to (LPVT) and (LPCT).

	Generic (both for VT and CT)	Generic (both for LPVT & LPCT)
accuracy	Non-linear. Saturates. Higher accuracy classes possible	Linear. No saturation. Extended range for high accuracy classes a correction factor could be necessary
logistics and design	features must be calculated for each protection, control or metering scheme	no need for calculations as there is no saturation and no need to load the transformer
burden	load in the Ω , $k\Omega$ range	load in the $M\Omega$ range
	Conventional VT	LPVT
cost	cost of VT >>> cost of LPVT	
isolation	galvanic isolation	no galvanic isolation
size	more room is required	smaller and lighter
secondary status	must be loaded or open-circuited	safe by design
	Conventional CT	LPCT
secondary status	safe if protected, if not must be loaded or short-circuited	safe by design

2.7 Technical consideration

- **Considering operation and maintenance**

Project leaders should bear in mind that operation and maintenance engineers should also be properly trained to exploit the benefits of the new systems. The introduction of LPCTs and LPVTs in the MV network will affect mainly two aspects of the usual operation and maintenance procedures: MV cable insulation testing and RMU wiring testing. It is important to work together with the technology suppliers to train the staff, to provide timely technical support. [28]

- **Technical consideration in wiring and cabling**

With the introduction of LPCTs and LPVTs, it is still possible to use these terminal blocks but we should bear in mind that, given the very low-voltage level of the signal on the secondary

side of the LPCT or LPVT, the connection quality becomes critical. Due to the low-power nature of the signal, it is also possible to introduce some innovations on the wiring schemes. The use of coaxial cables with BNC or TNC connectors or shielded twisted pair cables with RJ45 connectors is a convenient and cost-effective option that allows avoiding polarity errors in the wiring. To use these new wiring schemes, field crews would have to be trained and equipped with appropriate tooling and procedures to ensure that safety requirements are met and the tests are performed correctly. [28]

- **The choice of LPVTs and CTs**

The choice of LPVTs was quite obvious after analyzing the requirements as they had several relevant advantages, including size and price. In some solutions, they are already being supplied integrated into the RMUs.

2.8 Accuracy in LPVT and LPCT

The operation of Smart Grids in presence of Distributed Energy Resources has required the introduction of new technologies in power systems, like digital communication, a new type of switchgear, different network topologies, and the massive use of (LPIT) which are replacing with conventional (ITs).

The use of (LPITs) has allowed implementing many new operating and measurement functions, new performance and features are requested to the IT to accomplish real-time network control with the highest efficiency, speed, and accuracy. Very accurate energy and power measurements must be performed to correctly split the energy production revenues among them and for a proper accurate reactive energy injection into the grid. Reaching such accuracy in its measurement gets very challenging. This is what is requested for the new devices used as voltage sensors, the Low Power Voltage Transformers (LPVT). Usually, such devices reduce the phase-to-ground primary voltage to amplitudes of few volts. In such a case matching the existing requirements in terms of accuracy of the voltage measurement required for the (LPITs) to feature special accuracy classes (far better than those of the inductive voltage transformers. Moreover, it will be useful to power network and system designers and operators for selecting suitable (LPVTs) according to also to the accuracy requested for the voltage measurement. It arises that the accuracy class of the (LPVTs) used in a three-phase system strongly affect the error. [29]

IEC standards for low-power passive current transformers (LPCT) and low-power passive voltage transformers (LPVT) were established, the IEC 61869-10[30], and IEC 61869-11[31] respectively. The standard accuracy classes vary from 0.1 to 3.0. An accuracy class 0.2 or better in combination with a matching reading unit would make these new transformers suitable for revenue metering of commercial MV customers. The application of (LPVT) and (LPCT) with matching electronic measurement equipment for accurate revenue metering (less than 0.2) is introduced.

Recently, studying has been performed based on IEC 61869-10 and IEC 61869-11 by calculating and estimating errors concerning correlate the uncertainty affecting the measurement of the voltage with the accuracy class of the (LPVT).[32]

2.9 The new generation of medium current transformer (LPCT)

LPCT is a magnetic sensor with an integrated shunt providing a reduced voltage output which represents the primary current (Fig.2-9). LPCT protection chain includes LPCT with transmitting cable, Sepam relay, tripping coil, circuit breaker. LPCT technology is the technical answer to the evolution of relay technology that is now based on digital design. There is only one sensor for all service currents. Then there is no need to choose the rating of the primary current as for the conventional CTs. [33]

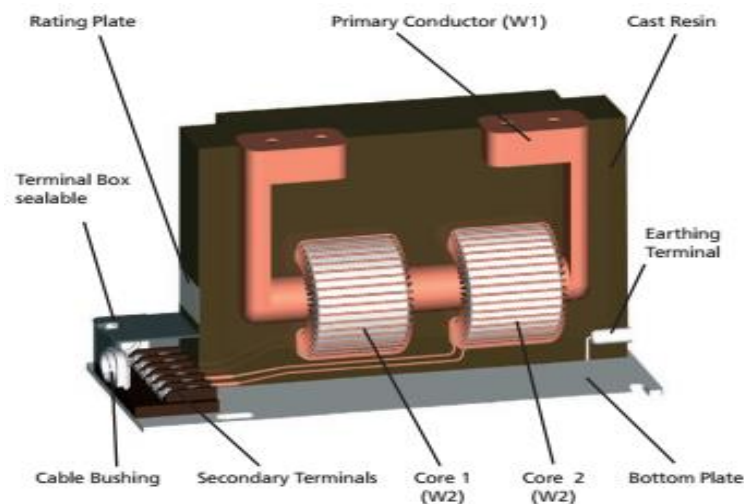


Fig. 2-9

- **Designer recommendation about using LPCT**

- To reduce the delivery time (less engineering, less lead time, less stock).
- To have a last-minute adaptation of a configured switching device or cubicle.
- To facilitate MV network evolution without any shutdown of the cubicle.

- **Choice limitations of the rated burden**

Especially for small rated primary currents, and high rated short-time thermal currents (I_{th}), the rated burden of a current transformer is limited due to the maximum permissible kAW-value (ampere-turns). In this case, the information should be requested from the manufacturer. If the rated burden of a current transformer is calculated according to the equation(2.4).

$$P_N = \frac{(AW)^2 \cdot Q_{fe} \cdot K}{I_{fe}} [VA] \quad (2.4)$$

Where:

AW	primary ampere-turns
Q_{fe}	iron cross section(mm ²)
K	constant
I_{fe}	ferromagnetic circuit(cm)

- **Rated primary and secondary current**

The value of the primary and secondary current indicates the performance rating of the transformer. A common practice is to use a secondary rated current of 1 or 5 A. The primary rated current depends on the network and is defined by the end-user.

- **Error limits**

The composite error for metering cores has to be higher than 10% to protect the connected metering devices in case of overcurrents. On the opposite, the composite error for protection cores at the rated accuracy limit of the primary current should be smaller or equal to 5% (5P) or 10% (10P) to secure the proper tripping of the connected protection devices.

- **Accuracy class**

This is the limit of the permissible percentage of current error at the rated current. In general, the limits of current error are calculated for a range between 1% up to 120% of rated current. (Fig.2-10) shows the relation of rated current and limitation of permissible current error for two classes 0.5 and 0.1 [33]

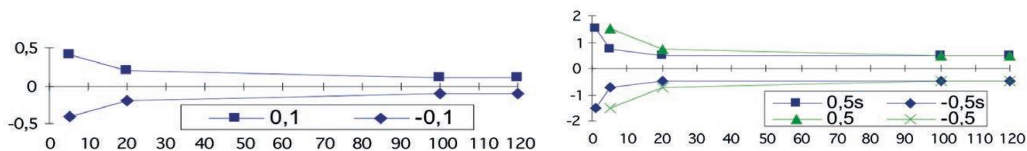


Fig. 2-10

LPCT is compliant with international standard IEC 60044-8[34], and therefore it has passed type and routine tests required by the standard. LPCT respects the same accuracy class with a wider range. Measuring accuracy class 0.5 protective accuracy class 5P. LPCT represents an evolution of the conventional CT. The conventional CT has been designed for electromechanical relays and therefore supplies a high power current output with a low range of application. Modern electronic relays have low input power requirement, so the LPCT which apply a voltage signal as secondary output with a wider range of application is the optimal solution. [35]

2.10 The new generation of medium voltage transformer (LPVT)

LPVT is the acronym for Low Power Voltage Transformer. LPVTs are sensor style VTs (resistive or capacitive dividers) as opposed to traditional iron core transformer style VTs. The output a secondary voltage between 0.2 and 4V and can be used in conjunction with an upconverter box to give a 120V output to protective relays and meters.

2.10.1 Passive LPVT

The low-power passive voltage transformer measures direct, alternating, and mixed voltages e.g. motor management, power quality analysis, and protection purposes. LPVTs domain of application is medium voltage installations like Static VAR Compensators or frequency converter installations. The passive LPVT(Fig.2-11) consists of a high voltage resistive divider (R1, R2), and capacitor divider (C1, C2) and epoxy resin tube as a surge protector. The voltage divider transforms the primary voltage at point (A) to a low voltage at point (a), which can be processed by the secondary system. The output cable and the input of the secondary system are compensated, leading to a wide frequency range.

The electromagnetic shielding ensures high EMC and makes the GSER 16 suitable for use in environments with heavy external interference and disturbance.

The GDT protects the secondary tap against high voltages since there is no galvanic isolation between the primary and secondary terminal. [36]



Fig. 2-11

- **Limits of voltage error and phase displacement**

The voltage error and phase displacement at the rated frequency shall not exceed the values given in the (tableIII) at any voltage between 80% and 120% of rated voltage and with burdens between 25% and 100% of the rated burden and a power factor of 0.8.

TABLE.III. voltage error and phase displacement at the rated frequency

Accuracy class	\pm voltage error(%)	\pm phase displacement
0.2	0.2	10
0.5	0.5	20
1	1	40

- **The rated thermal limiting**

The thermal limiting output of the residual winding shall be specified in volt-ampere (VA) about the secondary voltage with the unit power factor. The preferred values are given in the IEC-Standard. Since the residual windings are connected in an open delta circuit, these windings are only loaded under fault conditions. Therefore, a maximum duration of 8 hours, for example, can be chosen.

The rated voltage factor is determined by the maximum operating voltage depending on the system's grounding conditions. In single pole insulated transformers, it is common practice to use a rated voltage factor of 1.9 the rated voltage for a load-duration of 8 hours. The rated factor is defined as 1.2.UN for all other types. [37]

2.10.2 Active LPVT

The goal should be to guarantee that any LPVT or LPCT will be able to operate with an IED. IEC-60044[38] standard specifies the tests that are required for electronic instrument transformers from electrical safety. Moreover, Two main types of devices are distinguished, passive LPVTs, and active ones. A passive LPIT is an (LPIT that includes only passive components) while an electronic LPIT is an (LPIT that includes active components) .it differs from an electronic LPIT by the presence of a power source and of an active circuit that adjusts the transformers' output. The electronic voltage transformer measure direct, alternating, and mixed voltages with high accuracy e.g. motor management and power quality analysis. Its area of application is medium voltage installations, which require the voltage divider to be independent of the connected burden. The electronic voltage transformer is an alternative to conventional voltage transformers once the primary voltage contains DC components and/or higher frequencies. This system consists of a low-power passive voltage transformer (passive LPVT) and a buffer amplifier. The voltage divider inside the passive LPVT transforms the primary voltage U_p to a low voltage, which is processed inside the electronics. For this processing, the auxiliary power supply U_a is required. Various protection devices make sure no high voltages can damage the electronics and the secondary equipment since there is no galvanic isolation between the primary and secondary terminal.

The buffer amplifier makes the passive LPVT independent of the connected burden and allows the output signal to be fed into more than one secondary equipment, thus extending the performance of the passive LPVT. The intelligent electronic devices (IEDs) (Fig.2-12) that collect and process the measurements of the LPCTs and LPVTs are another important factor to ensure the success of MV distribution automation projects. Contrary to CTs and VTs, the output of low-power sensors can be wired to an IED utilizing a thin wire such as the ones that are used for communications. Some vendors are leveraging on this to propose new connector options such as (RJ45) connectors that could carry both the V and I signals of a given phase in a single connector. One of the main challenges is ensuring compatibility between LPVTs, LPCTs, and IEDs. The IEC-61869 includes specific safety and accuracy tests for LPCTs and LPVTs that will fill the existing gaps soon standard. [39]



Fig. 2-12

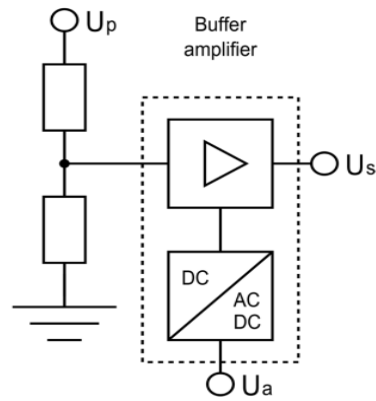


Fig. 2-13

2.11 LPVT (smart terminals)

For connection of polymeric MV cables to transformers, switchgear units (GIS and conventional), and motors, etc, Indoor and outdoor installation (Fig.2-14). The connector is entirely protected by a watertight conductive envelope connected to the earth.

Smart terminals features

- Continuous 250 A RMS overload 300 A RMS (8 hours per 24-hour period).
- operated when de-energized. Test by voltage detector through an inbuilt capacitive voltage divider.
- Single-core polymeric insulation (PE, XLPE, EPR...).copper or aluminum conductors.
- The semi-conducting screen either extruded or taped.
- the metallic screen of tape, wire, or poly lam type.
- Insulation voltage up to 24 kV (U_m).
- Conductor sizes: 16 to 120 sqmm.no need for special tools, no heating, taping, or filling.
- Vertical, angled, or inverted position. No minimum distance between phases.
- energizing may take place immediately after the connector is plugged into its bushing, dead-end plug...
- Individual clamping by stainless steel brace. The three phases may also be locked together and to the equipment by use of metallic. [40], [41]

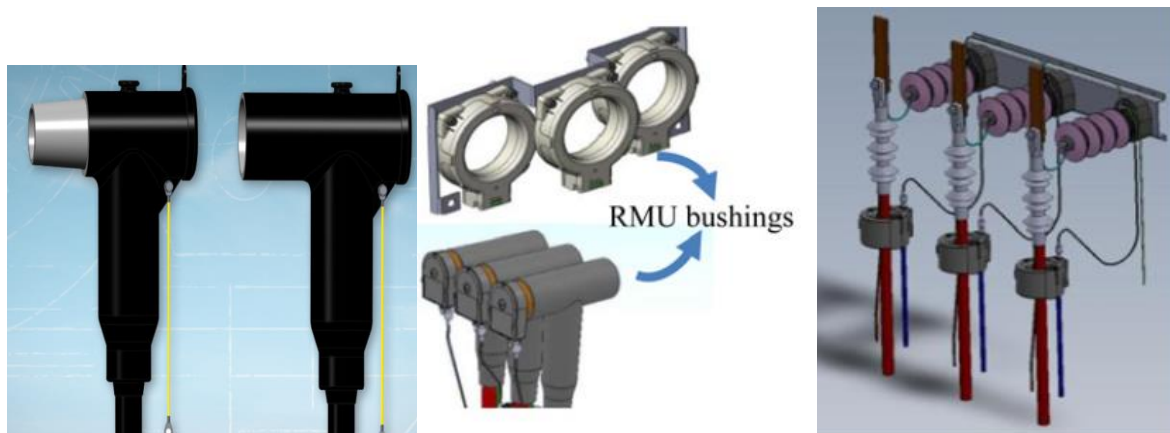


Fig. 2-14 Installation in AIS (right) and GIS (middle) RMUs and smart termination (left)

2.12 Insulations consideration

The engineer in charge of guiding the installation should pay special care to the selection of the position of the LPVT within the MV cable compartment. The LPVT should be installed in such a way that it will always respect that minimum distance. The same applies for all the cables that are used for the low-voltage signals RMU bushings on the secondary side of the LPVT and/or LPCTs.

The shield of the LPVT cable shall be connected to the ground only inside the sensor. In the case of voltage and current integrated sensors, a common shield is present, for both current and voltage sensors wires. Moreover, all of the LPVT shields shall be connected to the ground inside of the sensor. It is never allowed to use the ground eventually taken from the protection device for grounding sensors and/or cable shields. Also, the ground point of the capacitive divider shall be connected to the ground only inside the sensor. The ground eventually taken from the protection device cannot be used to ground the capacitive divider. [28]

The optimal installation location could be the bushing. Measuring current at the MV cable would require either disconnecting the MV cable or using a split-core CT/LPCT; besides this, it would also be necessary to pass the cable-shielding through the CT/LPCT.

2.13 Dielectric permittivity in LPITs

The Structure of LPITs is involved in dielectric (epoxy resin) characteristics. Because of the non-ideal characteristic behavior of dielectric, the frequency response in LPITs can be effected by leakage resistivity and frequency dependency of the permittivity. This paragraph will explain short comments about the impotence of dielectric spectroscopy and the polarization/relaxation phenomena. That induced in dielectric materials during and after the

application of imposing variable frequency or impulse signal. According to the LPVT instructor, it is better to understand the concept of dielectric and permittivity impact of the capacitor, in the following, short remind of capacitor instructor is presented.

The capacitor is a component that has the ability or “capacity” to store energy in the form of an electrical charge producing a potential difference (Static Voltage) across its plates, much like a small rechargeable battery. In its basic form, a capacitor consists of two or more parallel conductive (metal) plates which are not connected or touching each other but are electrically separated either by air or by some form of a good insulating material such as waxed paper, mica, ceramic, plastic or some form of a liquid gel as used in electrolytic capacitors. The insulating layer between a capacitor's plates is commonly called the Dielectric. when a capacitor is connected to an alternating current or AC circuit, the flow of the current appears to pass straight through the capacitor with little or no resistance.

The capacitance of a parallel plate capacitor (Fig.2-15), is proportional to the area, A in metres² of the smallest of the two plates and inversely proportional to the distance or separation, d (i.e. the dielectric thickness) given in meters between these two conductive plates.

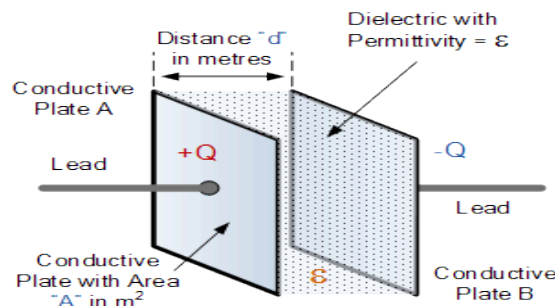


Fig. 2-15

The generalized equation for the capacitance of a parallel plate capacitor is given as

$$C = \epsilon \frac{A}{d}$$

where ϵ represents the absolute permittivity of the dielectric material being used. The permittivity of a vacuum, ϵ_0 is also known as the “permittivity of free space” has the value of the constant 8.84×10^{-12} Farads per meter. [42]

2.13.1 The dielectric of a capacitor

As well as the overall size of the conductive plates and their distance or spacing apart from each other, another factor that affects the overall capacitance of the device is the type of dielectric material being used (2.6). In other words the “Permittivity” (ϵ) of the dielectric. The dielectric material used is always an insulator. The various insulating materials used as the dielectric in a capacitor differ in their ability to block or pass an electrical charge. This dielectric material can be made from several insulating materials or combinations of these materials with the most common types used being: air, paper, polyester, polypropylene, Mylar, ceramic, glass, oil, or a variety of other materials.

The factor by which the dielectric material, or insulator, increases the capacitance of the capacitor compared to air is known as the Dielectric Constant, k and dielectric material with a high dielectric constant is a better insulator than a dielectric material with a lower dielectric constant. The dielectric constant is a dimensionless quantity since it is relative to free space. The actual permittivity or “complex permittivity” of the dielectric material between the plates is then the product of the permittivity of free space (ϵ_0) and the relative permittivity (ϵ_r) of the material being used as the dielectric. Practically, the permittivity of free space, ϵ_0 as our base level and make it equal to one, when the vacuum of free space is replaced by some other type of insulating material, their permittivity of its dielectric is referenced to the base dielectric of free space giving a multiplication factor known as “relative permittivity”, ϵ_r .

$$\text{Capacitance, } C = \frac{\epsilon_0 \epsilon_r A}{d} \text{ Farads} \quad (2.6)$$

Several factors can influence a capacitor instead of contracture parameters, all capacitors have a maximum voltage rating and when selecting a capacitor consideration must be given to the amount of voltage to be applied across the capacitor. If the applied voltage becomes too great, the dielectric will break down and arcing will occur between the capacitor plates resulting in a short-circuit, another factor which affects the operation of a capacitor is Dielectric Leakage. Dielectric leakage occurs in a capacitor as the result of an unwanted leakage current which flows through the dielectric material. Generally, it is assumed that the resistance of the dielectric is extremely high and a good insulator blocking the flow of the current. However, if the dielectric material becomes damaged due to excessive voltage or over temperature, the leakage current through the dielectric will become extremely high resulting in a rapid loss of charge on the plates and an overheating of the capacitor eventually resulting in premature

failure and thus aging of the dielectric. All in all, the conductive plates and their distance or spacing apart from each other in capacitor almost are constant parameters and do not change during operation but, the dielectric constant and relative permittivity are key to the operation of capacitors and the determination of the levels of capacitance achievable and both can be the state variables which must be considered. Permittivity and dielectric constant are two terms that are central to capacitor technology, the terms permittivity, and dielectric constant are essentially the same for most purposes.

The dielectric will also need to be chosen to meet requirements such as insulation strength - it must be able to withstand the voltages placed across it with the thickness levels used. It must also be sufficiently stable with variations in temperature, humidity, and voltage, etc.

Some materials have a very stable dielectric constant and can be used in high stability capacitors, whereas other dielectric materials enable very high levels of volumetric capacitance to be achieved. [43]

2.13.2 Specification factors in a capacitor

The Equivalent Series Resistance (ESR) of the capacitor, its Dissipation Factor (DF), loss tangent, and Quality Factor (Q) are all important factors in the specification of any capacitor. Factors like the ESR, dissipation factor, loss tangent and Q are important in many aspects of the operation of a capacitor and they can determine the types of applications for which the capacitor may be used. ESR, DF, and Q are all aspects of the performance of a capacitor that will affect its performance in areas such as frequency response. However, ESR and DF are also particularly important for capacitors operating in power supplies where a high ESR and dissipation factor, DF will result in a large amount of power being dissipated in the capacitor.

The equivalent series resistance or ESR of a capacitor has an impact on many areas where capacitors may be used. The resistor acts like any other resistor giving rise to voltage drops and dissipating heat.

The ESR of the capacitor is responsible for the energy dissipated as heat and it is directly proportional to the DF. When analyzing a circuit fully, a capacitor should be depicted as its equivalent circuit including the ideal capacitor, but also with its series ESR.

Although dissipation factor and loss tangent are effectively the same, they take slightly different views which are useful when designing different types of circuits. Normally the

dissipation factor is used at lower frequencies, whereas the loss tangent is more applicable for high-frequency applications. [44]

2.13.3 Dissipation factor and loss of tangent definitions

The dissipation factor is defined as the value of the tendency of dielectric materials to absorb some of the energy when an AC signal is applied.

The loss tangent is defined as the tangent of the difference of the phase angle between capacitor voltage and capacitor current for the theoretical 90-degree value anticipated, this difference is caused by the dielectric losses within the capacitor. The value δ (Greek letter delta) is also known as the loss angle.

$$\tan\delta = D.F \qquad \tan\delta = 1/Q \qquad \tan\delta = ESR/X_C \qquad (2.7)$$

Where:

δ = loss angle, DF = dissipation factor, Q = quality factor, ESR = equivalent series resistance,

X_C = reactance of the capacitor in ohms.

Actually, in LPVT epoxy resin is used for medium dielectric, and in this thesis is focused on epoxy resin Characteristic. Analysis of the epoxy resin is expected to reveal its dielectric characteristics in the frequency domain of the material under study. [45]

2.14 Frequency dependency to the permittivity

The dielectric properties of a material are associated with the response of the system to an applied electric field at microscopic and macroscopic levels. In the case of an ac driving field, these phenomena are expressed by the polarization and dielectric loss as a function of frequency. The frequency-dependent (ac), permittivity is defined through the linear relationship between the polarization and the ac driving field. It is tried to show how permittivity depends on the frequency and revile of why it will be necessary to analyze frequency response .in the following polarization in dielectric will be considered. [46]

- **The relationship between permittivity and resistance**

There is a relationship between the permittivity and the conductivity of a material, through the Kramers Kronig relations. The complex permittivity(2.8) is:

$$\epsilon^* = \epsilon' + j\epsilon'' \qquad (2.8)$$

Where ϵ' is the real (normal) permittivity, ϵ'' is the conductivity, ω is the radian frequency, and j is the usual sqrt (-1). Note that ϵ' and ϵ'' are both functions of frequency, and the Kramers Kronig relations show that the real and imaginary parts of a function aren't independent.[47]

Unfortunately to get the imaginary part from the real is needed to know the real part at all frequencies because the Kramers Kronig relations involve an integral over all frequencies. Numerically, we can use limited frequency data, but it is still needed to know the frequency variation, and there is an arbitrary constant representing the frequency ranges. Generally when a dielectric is subjected an alternating electric field the permittivity of the dielectric material is complex, because in a lossless dielectric the energy loss due to the propagation of electric field is zero, but in dielectric when there is the propagation of sinusoidal electric field through the medium some of the energy correspondings to this electric field gets converted to heat or some loss energy, so the real part of permittivity corresponds to the efficiency of a dielectric material to store the field energy and imaginary part accounts for the losses of energy due to the variation of ac electric field in the dielectric material. It indicates the Ohmic resistance of the material, for pure dielectric the imaginary part is zero, and increasing in imaginary part indicates the Ohmic loss. [48]

The real ϵ' (2.9) and imaginary ϵ'' (2.10) parts of dielectric constant are calculated using the following relation:

$$\epsilon' = c \cdot t / \epsilon_0 \cdot A \quad (2.9) \quad \epsilon'' = \epsilon' (\tan \delta) \quad (2.10)$$

Where: c = measured capacitance, t = thickness of the dielectric, ϵ_0 = permittivity of free space A = cross-sectional area of the electrode surface, $\tan \delta$ = dielectric loss

- **Permittivity variation**

The variation of the real part and imaginary part of the permittivity over a large range of frequency has been represented in (Fig2-16). The complex relative permittivity is defined by:

$$\epsilon_0 \cdot \epsilon^* = (\epsilon' - i\epsilon'')\epsilon_0 \quad (2.11)$$

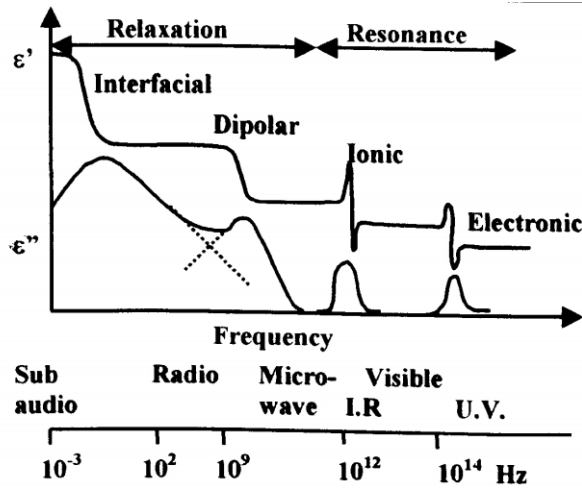


Fig. 2-16 Variation of the real and imaginary part of the permittivity over the frequency domain

The interest in working in the frequency domain is multiple. Most of the application of dielectric materials involves the response to harmonic signals of definite frequencies. Besides, measurements in the frequency domain lead to accurate results since signals can be obtained in a very narrow range of frequencies thus limiting the noise level recorded. [49]

The polarization is defined by the equation:

$$P(\omega) = \epsilon_0 x(\omega) \cdot E(\omega) \quad (1.12)$$

The frequency-dependent susceptibility is defined:

$$x^*(\omega) = x'(\omega) - ix''(\omega) \quad (1.13)$$

$\omega = 2\pi f$ (where ω is the circular frequency and f the frequency in Hertz) $f(t)$ is a real function of time that is equal to the discharge current after a step-down field, $x'(\omega)$ and $x''(\omega)$ components vary in-phase and quadrature respectively compared to the harmonic signal applied. From this data, other characteristics are accessible such as the impedance, Z^* and the capacitance, C^* that are useful for the interpretation of the data.[49]The following relations (2.14),(2.15) link them:

$$Z^*(\omega) = 1/(i\omega C^*(\omega)) \quad (2.14)$$

In parallel plate geometry, the capacitance is given by:

$$C^*(\omega) = \epsilon_0(X^*(\omega) + \epsilon_\infty) A/d \quad (2.15)$$

It can be seen the capacitor characteristics and dielectric components and complex permittivity in LPVT are frequency dependent. Studying and survey on frequency response analysis could

be the main way to identify the behavior of LPVT functionality. For this reason for finding frequency response we need to supply the wide spectrum of frequency but this method takes a lot of time unstable parameters and various test experiment conditions and effective parameters during a long time will appear unacceptable and unexpected errors. to cope with this problem Fast Procedure for Low Power Voltage Transformers (LPVT) is recommended, according to the specific feature of impulse signal and imply fast Fourier transformation (FFT) the frequency response can be achieved in acceptable approximation. The next Chapter contains the subjects to clarify these methods and relevant concepts.

CHAPTER 3

PROCEDURE

3 The procedure

Characterization and modeling of dynamic systems with impulse response test is a well-known procedure. The impulse frequency response test provides the dynamic system behavior for all the frequencies at the same time. This procedure is a one-time test compared to the sweep frequency test which has to be repeated for all desired frequencies.

So far, it is recognized as the important role of voltage and current measurement sensors. Also, it is known that factors and parameters which impact on accuracy and functionality of ITs. We have mentioned several thesis and surveys using impulse response for the recognition system and find out the unknown parameters. Several attempts and studies on some high light notes about conventional ITs (CT, PT, CVT) and the new generation (LPCT, LPVT) were represented. The importance of employed dielectric and value of permittivity and frequency dependency and influence parameters on accuracy was noted. In this chapter, the necessity of dynamic modeling and definition of (LPITs) as a system to purpose identification, the definition of features, frequency analysis, and responses will be present. Recognizing the model of LPITs helps to understand how the influence of quantities analysis could be effected on applications and responses of the LPITs model. Moreover, the model of LPVT will be considered and focused. Since the impulse signal has a very short time length and it is not recognizable to detect by data acquisition chain and for measure and computerize measurement values we have to use the data acquisition board. Moreover, working by data acquisition will be brought us some restrictions because of the limitation on the sample rate. Therefore, to reach a better resolution to detect signal it is better to use the proper model in the frequency domain and define LPVT as a system in the frequency domain. Theoretical subjects that are related to signals and systems and also control theory that will be helped to manifest LPVT behavior supplying impulse signal.

Actually, for impulse response analysis, the main considerations are the definition of suitable, valid model and exposition of systems, transfer function, and also impulse signal characteristic. To analyze in both time domain and frequency domain definition and specific consideration on Fast Fourier transformation (FFT) operation, convolution law, discrete Fourier transform (DFT) and discrete-time Fourier transform (DTFT) are inevitable. In the following, the new method based on approximation of impulse signal using the SINC function is presented. Moreover, the reasons that are helped to determine the frequency bound in this study will be

explained. Finally, Theoretical parts that are employed to calculate and reach to transfer function of LPVT will be clarified.

3.1 The dynamic model of LPVT

Representation of the LPVT model can aid in defining, analyzing, and communicating a set of concepts. Such this model is specifically developed to support the analysis, specification, design, verification, and validation of an LPVT as a system. One of the first principles of modeling is to clearly define the purpose of the model.

A System: consisting of interconnected components, built or evolved with the desired purpose.

What is a dynamical system?

Static vs. Dynamical model

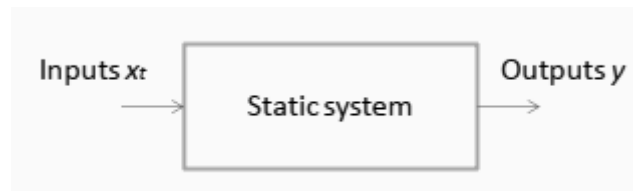


Fig 3-1. Static system: current inputs ==> outputs

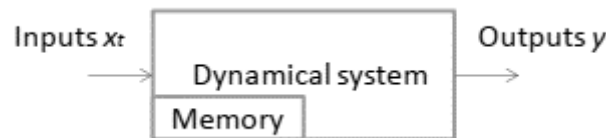


Fig. 3-2 Dynamical system: history + current inputs ==> outputs

Outputs depend on the present and past values of the inputs, Changes over time, sometimes called dynamic systems or sequential systems, and mathematically described with differential or differ.

In this study for simplifying, LPVTs are supposed as a static system without considering primary condition (memoryless). [50]

- **Linear and nonlinear system**

Generally, most systems are inherently nonlinear and time-varying. Nonlinear time-varying systems are very hard to deal with. Even though many of the systems may have nonlinear behavior characteristics, they can be approximated to be linear systems and they allow for

transform analysis. Besides, we are interested in systems that operate in the same manner every time we use them. Moreover, the systems which are assumed in this thesis must be independent of time. Linear time-invariant system analysis and design is the basis of present-day system analysis and design. Transfer functions associated with these systems are discussed. Also, the frequency analysis and other studying make it very achievable and understandable for the design of systems. The majority of the discussion in this chapter is on linear time-invariant systems. These allow that LPVT introduces for the transfer function. The study of the amplitude and phase-frequency responses of linear time-invariant systems is one of the important topics. [51]

Our study starts with a system that has an input and an output. It is symbolically represented by a block diagram shown below. The T inside the box is some transformation that converts the input signal $X(t)$ into the output signal $Y(t)$ and the system named linear system if satisfy two conditions: Principle of additivity and Principle of proportionality.[52]

$$y(t) = T[x(t)] \text{ (T maps } x(t) \text{ into } y(t)) \quad (3.1)$$

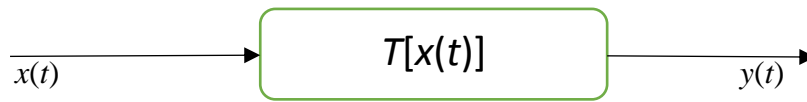


Fig. 3-3

- **Time-invariant and time-varying systems**

For any system of use, we like the system to respond every time the same functionality. That is, if we switch today or tomorrow, the system should respond the same. Such a system is called a time-invariant system. Mathematically view, if the response of system is $y(t)$, (3.1) to the input $x(t)$, i.e. $y(t) = T[x(t)]$, (Fig.3-3) then the system is called a time-invariant or a fixed system if $T[x(t - t_0)] = y(t - t_0)$, otherwise, it is a time-varying system. If the system is a linear system and time-invariant it will name (LTI) system. [51]

Consider a system with a scalar input signal $x(t)$ and a scalar output signal $y(t)$ (Fig. 3-3). It is considered the LPVT as a time-invariant system if its response to a certain input signal does not depend on absolute time. It is said to be linear if its output response to a linear combination of inputs is the same linear combination of the output responses of the individual inputs. Furthermore, and also, it is said to be causal if the output at a certain time depends on the input up to that time only. Therefore, LPVTs can be considered as a linear, time-invariant, causal system that can be presented such a transfer function model.

3.2 Unit impulse function

The unit impulse function is also known as the Dirac delta function, which is often referred to as delta function is defined as:

$$\delta(t) = 0, t \neq 0$$

$$\int_{-\infty}^{\infty} \delta(t) dt = 1 \quad \delta(t) = \begin{cases} 0, & \text{if } t \neq 0 \\ \infty, & \text{if } t = 0 \end{cases} \quad (3.2)$$

The delta function can be evolved as the limit of the rectangular pulse as:

$$\delta(t) = \lim_{\Delta \rightarrow 0} P_{\Delta}(t) \quad (3.3)$$

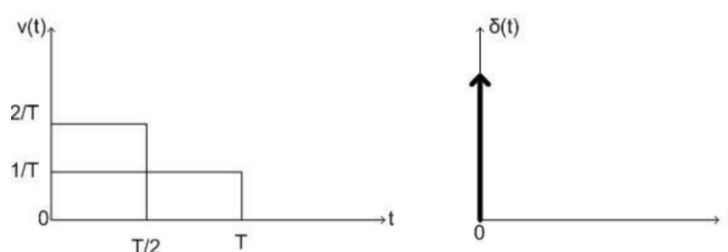


Fig. 3-4

As the width $\Delta \rightarrow 0$, the rectangular function converges to the impulse function $\delta(t)$ with an infinite height at $t = 0$, and the total area remains constant at one.[51]

Some Special Properties of the Impulse Function:

3.2.1 Sampling property

The sampling theorem plays a crucial role in modern digital signal processing. The theorem concerns the minimum sampling rate required to convert a continuous-time signal to a digital signal, without loss of information. Computerizing the analog data or measurement values from LPVT and other devices in an experimental setup using a data acquisition board (DAQ) is necessary. The main function of DAQ is analog to digital converter (ADC) which works based on sampling.

Mathematically, the impulse signal has several properties, in this part, it is considered the role of impulse in the sampling of input values. Therefore, we assume that an arbitrary signal $x(t)$ is multiplied by a shifted impulse function(Fig.3-5), the product is given by:

$$x(t)\delta(t - t_0) = x(t_0)\delta(t - t_0) \quad (3.4)$$

Implying that multiplication of a continuous-time signal and an impulse function produces an impulse function, which has an area equal to the value of the continuous-time function at the location of the impulse.[53] Also, it follows that for $t_0 = t$.

$$x(t)\delta(t) = x(0)\delta(t) \quad (3.5)$$

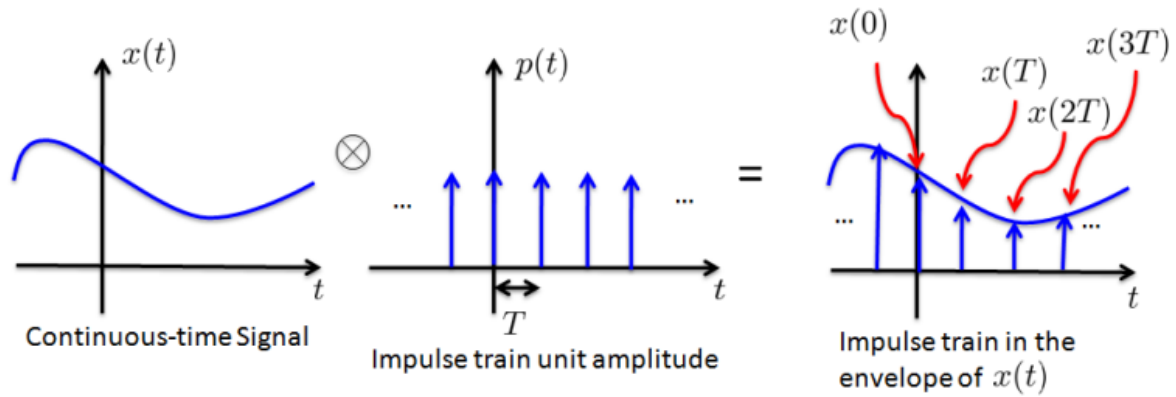


Fig. 3-5

3.3 Study of impulse response system identification

The impulse response test provides dynamic system behavior for all the frequencies at the same time. This procedure is a one-time test compared to the sweep frequency test which has to be repeated for all desired frequencies. This thesis discusses one of the most useful techniques for experimental structural impulse response testing-one based upon excitation of the LPVT structure with an impulsive signal. In many situations, this is the simplest and fastest of the various techniques commonly used. However, the nature of the excitation and response signals in the impulse technique requires special signal processing techniques if accurate impulse response measurements are to be obtained.

In system identification, different methods are often classified as parametric or nonparametric methods. In the parametric method, the system is considered as a parametric model to be estimating. For non-parametric methods, in no parametric model, the result of the identification is given as a curve or a function.

One of the non-parametric methods is the impulse response analysis. This approach is a dynamic simulation. This approach is based on choosing a Dirac function $\delta(t)$ as input, and as a result, the output will be equal to the impulse response. The behavior of LTI systems is completely characterized by their impulse response. We would like to attain the impulse response of an LTI system, described by the impulse response $h(t)$.[54]

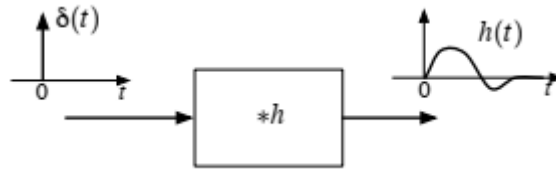


Fig. 3-6

For input at a time ($t = \tau$): The impulse response of a linear system $h_\tau(t)$ is the output of the system at time t to an impulse at time τ . This can be written as $h\tau = H(\delta\tau)$, (Fig.3-6), (Fig.3-7)

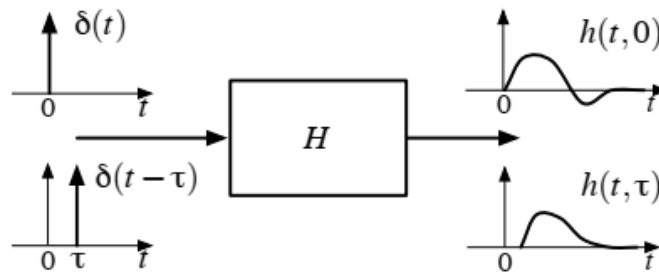


Fig. 3-7

- **Superposition integral**

We can write a signal $x(t)$ as a sample of itself(3.6). This means that $x(t)$ can be written as a weighted integral of δ functions.

$$x(t) = \int_{-\infty}^{\infty} x(\tau)\delta_\tau(\tau)d\tau \tag{3.6}$$

Applying the system H , (Fig.3-7)to the input $x(t)$:

$$y(t) = H(x(t)) \tag{3.7}$$

$$= (\int_{-\infty}^{\infty} x(\tau)\delta_\tau(t)d\tau) \tag{3.8}$$

If the system obeys extended linearity we can interchange the order of the system operator and the integration:

$$y(t) = \int_{-\infty}^{\infty} x(\tau)H(\delta_\tau(t))d\tau \tag{3.9}$$

The impulse response is:

$$h_{\tau}(t) = H(\delta_{\tau}(t)) \quad (3.10)$$

Substituting for the impulse response gives an output (3.11). Moreover, we can consequently compute the corresponding output $y(t)$ for any input. The impulse response is thus a complete characterization of the system. [55]

$$y(t) = \int_{-\infty}^{\infty} x(\tau)h_{\tau}(t)d\tau \quad (3.11)$$

However, a Dirac function cannot be realized in practice, while an impulse is a difficult concept to imagine, it represents the limit case of a pulse made infinitely short in time, and an approximation has to be used. As a consequence, the impulse response of a system is its output when presented with a brief signal, as an impulse. [54]

It is well known that a linear, time-invariant, the causal signal can be described by its impulse response or its weighting function $x(\tau)$. This system must be identified and characterize according to input and output data, and then can be described by its impulse response (or weighting function)

This is a superposition integral. The values of $x(\tau)h(t, \tau)d\tau$ are super-imposed (added up) for each input time τ . [55]

3.4 Definition of transfer function using impulse response

Theoretically, any linear discrete-time system can be fully described in the time domain by the impulse response $h(t)$. The $h(t)$ describes the response of the system to the infinitely fast unit impulse, which is also referred to the as Dirac delta function. The impulse response cannot be acquired experimentally with proper resolution using computer analysis and processing. For an LTI system, the input $X(j\omega)$ and output $Y(j\omega)$ signal in the frequency domain is related via the frequency response $G(j\omega)$ (transfer function), which is the FFT of the impulse response $h(t)$. [56]

$$F(h(t)) = \frac{F(y(t))}{F(x(t))} = \frac{Y(j\omega)}{X(j\omega)} \quad (3.12)$$

Where F is the symbol for FFT. Therefore, the output signal in the frequency domain $Y(j\omega)$ (2.13) , and in the time domain $y(t)$, can be calculated as:

$$Y(j\omega) = G(j\omega). x(j\omega) = F[h(t)] . F[x(t)] \quad (3.13)$$

$$y(t) = F^{-1}[Y(j\omega)] \quad (3.14)$$

Where F^{-1} stands for *IFFT* (3.14). This transformation approach for the calculation of the output of a linear system is theoretically the same as convolution's approach which is explained in the next paragraph. This is one of the main objects in which we can find the correct and proper impulse response for describing the LPVT transfer function. [56]

3.4.1 Convolution integral

If H is time-invariant, this written a more simple form of a convolution integral (3.16). The input and output of an LTI system are related by convolution sum/integral (in discrete signals summation uses instead of integral) (3.17). The response of an LTI system is completely characterized by its impulse response $h(t)$. Given the impulse response, we can find the output for any input signal waveform using convolution.[57]

$$y(t) = \int_{-\infty}^{\infty} x(\tau)h(t - \tau)d\tau \quad (3.16)$$

$$y(t) = (x * h)(t) \quad or \quad y = x * h \quad or \quad y(t) = x(t) * h(t) \quad (3.17)$$

- **Convolution property at impulse and frequency response**

In the time domain, two signals are convolved then the Fourier transform of the convolution is just the product of the two original Fourier transforms (3.19). In other words, convolving signals in the time domain is equivalent to multiplying their Fourier transforms in the frequency domain. Thus, what appears in the time domain to be a complicated operation, will be simple if it considers in terms of the frequency domain. As with some others, this property is derived by using the definition of the Fourier transform and manipulating the expression. But, now we will have two integrals – one for the transform and one for the convolution.

$$\begin{aligned} F\{x(t) * h(t)\} &= F\left\{\int_{-\infty}^{\infty} x(\tau)h(t - \tau)d\tau\right\} \\ &= \int_{-\infty}^{\infty} \left(\int_{-\infty}^{\infty} x(\tau)h(t - \tau)d\tau\right) e^{-j\omega t} dt \end{aligned} \quad (3.19)$$

$$= \int_{-\infty}^{\infty} x(\tau) \left(\int_{-\infty}^{\infty} h(t - \tau)e^{-j\omega t} dt\right) d\tau \quad (3.20)$$

by changing the order of integration:

$$= \int_{-\infty}^{\infty} x(\tau) \left(\int_{-\infty}^{\infty} h(u) e^{-j\omega(u+\tau)} du \right) d\tau \quad (3.21)$$

by a change of variables to $u = t - \tau$

$$= \left(\int_{-\infty}^{\infty} x(\tau) e^{-j\omega\tau} d\tau \right) \left(\int_{-\infty}^{\infty} h(u) e^{-j\omega u} du \right) \quad (3.22)$$

$$= X(\omega)H(\omega)$$

This property is called the multiplication property or the modulation property. Recall that for an LTI system with impulse response $h(t)$, if we apply the input $x(t)$ then the output is $y(t)$. [58] So, we can find what this output (3.23) looks like in the frequency domain. From the convolution property, we immediately see that:

$$y(t) = x(t) * h(t) \quad Y(\omega) = X(\omega) \cdot H(\omega) \quad (3.23)$$

Convolution of two signals in the time domain is equal to the IFFT of the product of their FFTs. As we have seen, a Dirac function delta, $\delta(t)$ is needed as input and output will be equal to the weighting function $x(t)$ of a system. While this is impossible in practice to realize an ideal impulse, it is a useful concept as an idealization. Therefore, an approximate impulse must be used. Thus, we calculate the weighting function and the responses to the approximate impulse we have considered above and various values of impulse duration. In the following the method which is used to determine the approximation impulse signal will explain. [58]

As it is seen, In this thesis LPVT system must be identified and characterize according to input and output data which can be described by its impulse response, by having impulse response of LPVT, it is possible to achieve analysis the behavior of LPVT corresponding arbitrary input signals in a different range of frequency to recognize different responses to other signals and harmonic waveform using convolution property in the system under survey.

- **Impulse response definition using convolution**

Consider an LTI system (Fig.3-8) with impulse response $h(t)$ and input signal $x(t)$:

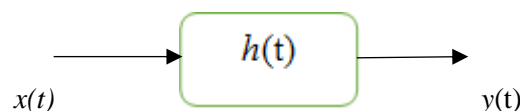


Fig. 3-8

For instance: suppose that input $x(t) = e^{st}$, then the output is given by:

$$y(t) = h(t) * x(t) = \int_{-\infty}^{\infty} h(\tau)x(t - \tau)d\tau \quad (3.24)$$

$$= \int_{-\infty}^{\infty} h(\tau)e^{s(t-\tau)}d\tau \quad (3.25)$$

$$= \left[\int_{-\infty}^{\infty} h(\tau)e^{-e\tau}d\tau \right] e^{st} = H(s)e^{st} = H(s).x(t) \quad (3.26)$$

Where $H(s)$ is defined as:

$$H(s) = \int_{-\infty}^{\infty} h(\tau)e^{-st}d\tau \quad (3.27)$$

The function $H(s)$ is known as the *transfer function* of the continuous-time LTI system (Fig 3-9). Note that $H(s)$ is defined by the impulse response $h(t)$, and is a function in s (independent of t). Therefore, $H(s)x(t)$ can be regarded as a scalar $H(s)$ multiplied to the function $x(t)$.

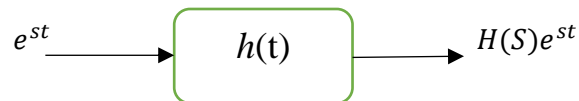


Fig. 3-9

Therefore, using the definition of the transfer function, we show that:

1. e^{st} is an eigenfunction of any continuous-time LTI system, and
2. $H(s)$ is the corresponding eigenvalue.

If we specialize in the periodic complex exponentials of the $e^{j\omega}$ by substitute $s = j\omega$ then

$$H(s) \text{ for } s = j\omega \xrightarrow{\text{yields}} H(j\omega) = \int_{-\infty}^{\infty} h(\tau)e^{-j\omega\tau}d\tau \quad (3.28)$$

$H(j\omega)$ is called the *frequency response* (3.28) of the system.[53]

A large family of electrical apparatuses works in the standard frequency range (50 HZ±5%) but because of the presence of harmonics and unexpected signals such as kind of noises and also because of the importance of power quality parameters, many industrial producers have been considering to determine frequency range which the devices can have proper functionality. Therefore, by frequency response studying and finding out the behavior. The reaction to different frequencies from a definite spectrum and bandwidth result, give us valuable information to design and improve quality level and development.

Thus, although all the signals compose in the time domain, they are distinct in the frequency domain. With some basic frequency domain processing, it is straightforward to separate signals and even tune in or extract the frequency we're interested in. The frequency-domain representation of a signal allows us to observe several characteristics of the signal that are either not easy to see, or not visible at the signal in the time domain.

For instance, frequency-domain analysis becomes useful when we are looking for the cyclic behavior of a signal, also shows how the signal's energy is distributed over a range of frequencies. Moreover, it includes information on the phase shift that must be applied to each frequency component to recovering the original time signal with a combination of all the individual frequency components.

3.4.2 FFT and IFFT concept

A signal can be converted between the time and frequency domains with a pair of mathematical operators called a transform. Fourier transform, which decomposes a function into the sum of numbers of sine waves frequency components. The spectrum of frequency components is the frequency domain representation of a signal. Fourier series, the signal is the continuous and finite duration in the time domain, but in the frequency domain, it is discrete and infinite duration. The inverse Fourier transform converts the frequency domain function back to a time function. so, it supports the duality properties as well. The Fourier transform is most used in analyzing analog systems.

Here the definitions of the forward (3.29) and inverse (3.30) transforms are repeated by equations. For the FT, both the time variable t and frequency variable are continuous-valued and vary from $-\infty$ to $+\infty$ the transform equations are:

$$X(\omega) = \int_{-\infty}^{\infty} x(t)e^{-j\omega t} dt \quad \text{forward transform} \quad (3.29)$$

$$x(t) = \frac{1}{2\pi} \int_{-\infty}^{\infty} X(\omega)e^{j\omega t} d\omega \quad \text{invers transform} \quad (3.30)$$

The DFT and it's inverse function allow you to compute the Discrete Fourier transform (DFT) of a signal and the inverse of this transform respectively. The DFT is widely used in digital computations, because of a fast algorithm called the FFT (fast Fourier transform) for computing the DFT. in this thesis FFT function is widely used in the LabVIEW program which is explained in next chapter.[58]

The DFT is used in the case of a finite-duration, discrete-time signal, $x[0]; x[1]; \dots; x[N-1]$. The DFT $X[0]; X[1]; \dots; X[N-1]$ is also finite-duration and discrete frequency (3.31). The definitions of the forward and inverse DFT are:

$$X[k] = \sum_{n=0}^{N-1} x[n]e^{-jk\omega_0} \quad k = 0,1,2, \dots, N-1 \quad (3.31)$$

$$x[n] = \frac{1}{N} \sum_{k=0}^{N-1} X[k]e^{jk\omega_0 n} \quad k = 0,1,2, \dots, N-1 \quad (3.32)$$

In this thesis all transfer which are used in the frequency domain. It will be used a discrete form of a signal, because of using digital computing in the data acquisition chain in all measurements. Sampling the sim-impulse signal that it is designed according to the frequency bandwidth that we are defined, and also the sample per channel corresponding to data acquisition board, give us the valuable data which can use to determine output response of LPVT under test. The test procedure is explained completely in the next chapter.

3.5 Sinc function as an impulse signal

To measure voltage in-network, smart grid, and industrial field the new generation of LPVTs is deployed. LPVTs in both active and passive configurations are progressively utilized for their small size, bandwidth (up to KHZ's), and the accurate operation for measurement purposes. To the characterization of LPVTs, it is used impulse response and sweep Frequency Response tests as well-known methods in the literature. This is typically performed in terms of ratio and phase displacement to be aligned with the Standard IEC 61869-6 [59]. For a dynamic system that we study on it, the range of frequency includes the power quality frequency rang. The sweep frequency response test characterizes dynamic systems by applying each frequency separately. This procedure is a one-time test compared to the sweep frequency test which has to be repeated for all desired frequencies. This kind of test is time-consuming compared to the impulse response test as it is a series of consequent tests for each frequency. Limitations imposed by impulse response test, such as slow rate of impulse signal and impulse response signal detection techniques, makes sweep frequency response test more feasible even if it is time-consuming.

In this thesis, it is started from the impulse response idea to present a new test signal to test capacitive low-power voltage transformers (LPVTs) in the power quality frequency range (50 Hz - 2.5 kHz). This frequencies spectrum can be approximated by acceptable and high

accuracy signal. Such a signal, detailed, is a rectangular window in the frequency domain, which results in a sinc signal in the time domain [60], [61].

In this thesis, the Sinc Response, in comparison to impulse response is introduced as an improvement of impulse response test with specified limited range of frequency but with a high resolution detected response.

The main problem in capacitive LPVT characterization with impulse response test is the short pulse width of impulse response and technical limitations for detecting such a short width signal. This limitation is imposed by a limited range of sampling frequency for Analog to Digital Converters (ADC) in the data acquisition board. The resolution of the measured impulse response of the signal should be high enough to detect the slight frequency dependency of a capacitive LPVT, but the frequency dependency of LPVT is very small and not zero. There are quasi-ideal sensors and non-ideal. The sources of non-ideally in capacitive LPVTs are the frequency dependency of the primary capacitance dielectric permittivity and the resistive leakage of the primary capacitance which is explained in the previous chapter. The solution we are approached in this thesis to overcome the mentioned challenge is using a normalized Sinc signal instead of an impulse signal.

3.6 Sinc function properties

In this part, some definitions and theorem with mathematical point of view that related to sinc function are represented and also by using example concerning duality in FFT the main approach to transfer rectangular signal (frequency spectrum) to sinc function as an impulse response will depict.

- **Sinc function definition**

The normalized sinc function (3.33) is defined to be:

$$\text{sinc}(x) = \frac{\sin x}{x} \quad (3.33)$$

This function is used in signal processing, understanding of the graphs of $\sin(x)$ and $1/x$ together is learned us to sketch a graph of $\text{sinc}(x) = \sin(x) \cdot 1/x$ because:

$$\lim_{x \rightarrow 0} \frac{\sin x}{x} = 1 \quad (3.34)$$

We know that $\text{sinc}(0) = 1$

Because of $\sin(x)$ oscillates between positive and negative values, $\text{sinc}(x)$ will do so as well. Except at $x = 0$, the x -intercepts of the graph of $\text{sinc}(x)$ will match those of $\sin(x)$.

We know that $-1 \leq \sin(x) \leq 1$, so it must be true that:

$$-\frac{1}{x} \leq \frac{\sin x}{x} \leq \frac{1}{x} \quad (3.35)$$

The graph (Fig.3-10) of $\text{sinc}(x)$ moves up and down between the graphs of $1/x$ and $-1/x$.

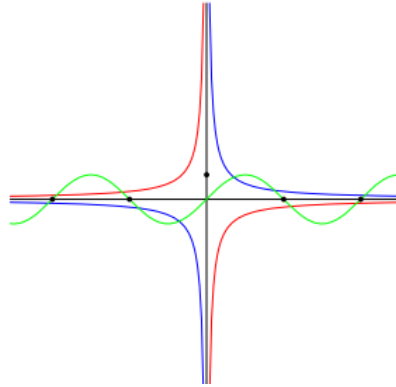


Fig. 3-10. The graphs of $\sin(x)$ (green), x (blue) and $-x$ (red)

In drawing the graph of $\text{sinc}(x)$ we start by superimposing the graphs of $\sin(x)$, $1/x$, and $-1/x$ (Fig.3-10).

When $x < 0$, both $1/x$ and $\sin(x)$ are negative, so their quotient is positive; $\text{sinc}(x)$ turns out to be an even function. By knowing this, (Fig.3-11) is shown the graph of $\text{sinc}(x)$ function. [62]

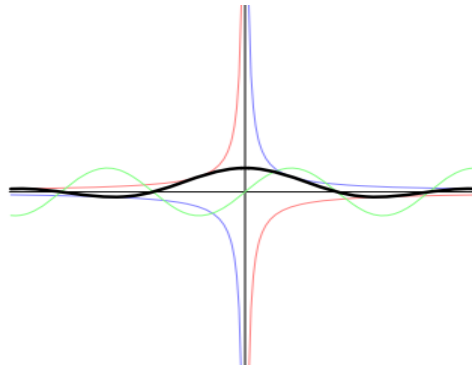


Fig. 3-11. The graph of $\text{sinc}(x)$

- **Types of sinc function**

Two sinc functions (Fig.3-12) we have: the ordinary sinc (un-normalized), (3.36a) essentially $\sin\theta/\theta$ which extends (from $-\infty$ to ∞) and has equally spaced zero crossings which are depicted (Fig.3-11), and the Dirichlet sinc (normalized) (3.36b), which is periodic and also has equally spaced zero crossings. Dirichlet sinc of order N is defined as:

$$\text{sinc}(x) = \frac{\sin x}{x} \qquad \text{sinc}(\pi x) = \frac{\sin(\pi x)}{\pi x} \qquad (3.36)$$

a- Un-normalized

b- normalized

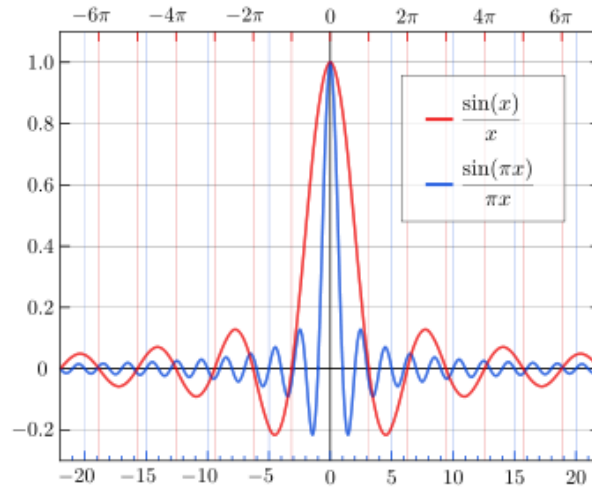


Fig. 3-12. The normalized sinc (blue) and un-normalized sinc function (red) shown on the same scale

The zero crossings of the un-normalized sinc are at non-zero integer multiples of π , while zero crossings of the normalized sinc occur at non-zero integers. Therefore, the sinc function oscillates with period 2π and decays with increasing t .

Thus, its value is zero at $(n\pi, n = \pm 1, \pm 2 \dots)$. It is an even function of t .

The local maxima and minima of the un-normalized sinc correspond to its intersections with the cosine function. [63]

- **Scale change theorem**

It is represented as a simple definition of sinc function. Actually, for changing rectangular spectrum or signal to sinc function the scale change theorem and symmetry or duality theorem should be considered, the scale change theorem states as:

$$F[x(at)] = \int_{-\infty}^{\infty} x(at)e^{-j\omega t} dt = \frac{1}{|a|} X\left(j\frac{\omega}{a}\right), a \neq 0 \qquad (3.37)$$

This (3.37) can be shown by considering the two possibilities, $a > 0$ and $a < 0$. For $a < 0$, by using the change of variable $\beta = at$ in the integral expression, we have:

$$F[x(t)] = \int_{-\infty}^{\infty} x(\beta)e^{-j\left(\frac{\omega}{a}\right)\beta} \left(\frac{1}{a}\right) d\beta \qquad (3.38)$$

$$= \left(-\frac{1}{a}\right) \int_{-\infty}^{\infty} x(\beta) e^{-j\left(\frac{\omega}{a}\right)\beta} d\beta \quad (3.39)$$

$$= \frac{1}{|a|} \int_{-\infty}^{\infty} x(\beta) e^{-j\left(\frac{\omega}{a}\right)\beta} d\beta = \frac{1}{|a|} X\left(j\frac{\omega}{a}\right) \quad (3.40)$$

When a is a negative number, $a = |a|$. For $a > 0$, the proof similarly follows. The scale change theorem states that timescale contraction or expansion corresponds to the frequency-scale expansion or contraction. [64]

- **Symmetry or duality theorem**

Duality theorem represents the concept of switch between time domain and frequency domain using Fourier transform (Fig.3-13) shows this concept.[64]

$$x(t) \leftrightarrow X(j\omega) \rightarrow X(t) \leftrightarrow 2\pi x(-j\omega) \quad (3.41)$$

Starting with the expression for $2\pi x(t)$ and changing the variable from t to $-t$ (3.42), we have:

$$2\pi x(t) = \int_{-\infty}^{\infty} X(j\omega) e^{j\omega t} d\omega \rightarrow 2\pi x(-t) \quad (3.42)$$

$$= \int_{-\infty}^{\infty} X(j\omega) e^{-j\omega t} d\omega \quad (3.43)$$

By Interchanging (3.44) t and $j\omega$ the result is:

$$2\pi x(-j\omega) = \int_{-\infty}^{\infty} X(t) e^{-j\omega t} \quad (3.44)$$

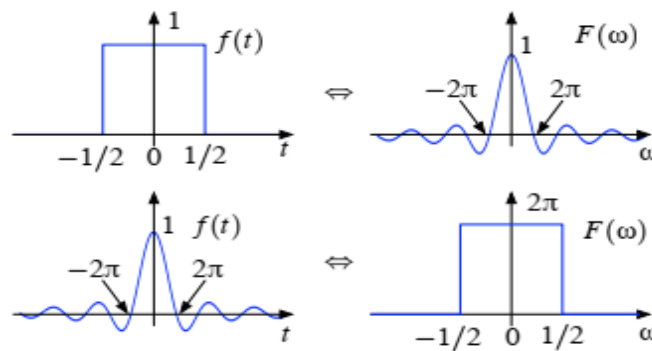


Fig. 3-13

3.7 Power quality frequency range

In this thesis, it is considered that the analog sinc function Fourier Transform as a bandlimited pulse (window) which represents a fixed value for all frequency components magnitudes (like an ideal impulse signal) but with a fixed range of frequency. The frequency range for the sinc function that to be used in the text form, which is fixed from 50 Hz to 2.5 kHz, concerns the power quality frequency range in power networks. As it is seen in the majority system like the smart grid, we have scattered distribution applications of photovoltaic and wind generators etc.... Where converters and power electronics apparatus works instead of alternators and conventional transformer systems. For instance, the large use of power inverters for inter-connecting large photovoltaic plants to the grid has led to the injection of high order harmonics, which can interfere with industrial frequency component or among them to give rise to intermodulation. In these power electronics convertors because of using switching techniques in these circuits and also because of the commutation phenomenon in the switching process, it is raised the main source to generate and inject the harmonics to grids and other devices (measurement devices and sensors). Thus, in the 50Hz (nominal frequency) system the higher frequency is generated and injected. These harmonics mostly are coefficients of the 50Hz and seriously can affect power quality. So, electrical devices, specifically sensors and measurement equipment must be tested and analyzed at a higher frequency and survey the behavior and changing functionality and their parameters impacted cause higher frequency than nominal frequency (50 Hz). Therefore, according to power quality standards [60], This is needed that such components be correctly and accurately measured to let such systems to run under real-time feedback control and it is considered to design the sinc function in this thesis we implement input spectral components (fig.3-14) are determined in the frequency range between 50 to 2.5 kHz by 50 Hz resolution.

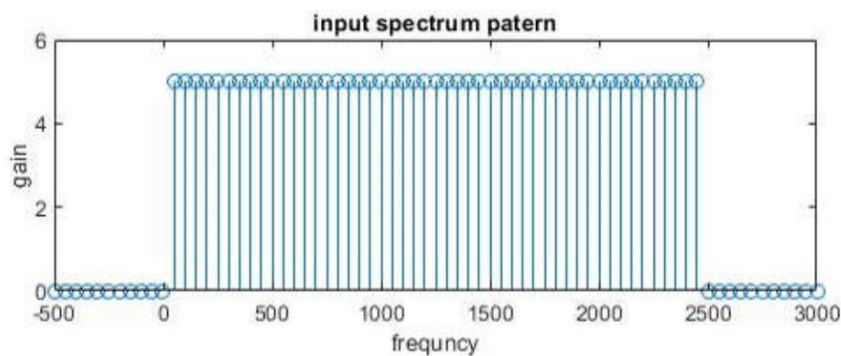


Fig. 3-14

3.8 Design the sinc signal

As we know, the sweep frequency response test characterizes dynamic systems by applying each frequency separately, this type of test is time-consuming compared to the impulse response test. There are a series of consequent tests for each frequency.

In this thesis, it is represented a new test signal to test capacitive low-power voltage transformers (LPVTs) in the power quality frequency range (50 Hz – 2.5 kHz). A signal, detailed in this chapter, is a bandlimited signal (rectangular window) in the frequency domain, which results in a sinc signal in the time domain. The Sinc Response, in comparison to impulse response, is introduced as an improvement of impulse response test with specified limited range of frequency but with a high resolution detected response.

In light of that desired frequency-domain signal, the sinc function is designed in the time domain.

For this purpose, it is necessary to pay attention to the mathematical view to attain the sinc function which is desired to imply in experimental tests, such as amplitude of window frequency range, determining the crossing points in sinc function, the number of lobes and amplitude of the main lobe in sinc function. Therefore, understanding the signal system concepts and techniques such as FFT, DTFT, and inverse FFT, DTFT is inevitable.

- **Frequency Interval/Resolution**

Frequency resolution is determined only by the length of the observation interval, whereas the frequency interval is determined by the length of the sampling interval and covered frequency interval.

$$F_{res} \sim \frac{1}{NT} \quad [Hz] \quad \Delta F = N\Delta F_{res} = \frac{1}{T} = F_S \quad [Hz] \quad (3.45)$$

- Increase sampling rate → Expand frequency interval,
- Increase observation time → Improve frequency resolution.

3.8.1 DTFT

The DTFT is a frequency-domain representation for a wide range of both finite and infinite-length discrete-time signals $h[n]$. The DTFT is denoted as frequency spectrum $H(e^{j\omega})$, which shows that the frequency dependence always includes the complex exponential function $e^{j\omega}$. The Operation of taking the Fourier transform of a signal will become a common tool for analyzing signals and systems in the frequency domain. For each value of ω over the domain $-\pi < \omega \leq \pi$. for each value ω replaces a function of a discrete-time index n (a sequence) by a

periodic function of the continuous frequency variable ω . By this transformation, the time-domain representation $h[n]$ is replaced by the frequency-domain representation $H(e^{j\omega})$, and vice versa. We need the ability to go back from the frequency-domain representation to the time-domain representation. That is, we need an inverse transform that recovers the original $h[n]$ from $H(e^{j\omega})$. [64]

$$H(e^{j\omega}) = \sum_{n=-\infty}^{\infty} h[n]e^{-j\omega n} \quad (3.46)$$

Discrete-time Fourier transform

$$h[n] = \frac{1}{2\pi} \int_{-\pi}^{\pi} H(e^{j\omega})e^{j\omega n}d\omega \quad (3.47)$$

inverse DTFT

We want to continue the development of the DTFT by studying a general expression for performing the inverse DTFT. The DTFT $H(e^{j\omega})$ is a function of the continuous variable ω , so an integral (3.47) for normalized frequency ω is needed to transform $H(e^{j\omega})$ back to the sequence $h[n]$.

3.8.2 Bandlimited pulse (window pulse)

Ordinarily, we define a signal in the time domain, but the inverse DTFT integral enables us to define a signal in the frequency domain by specifying its DTFT as a function of frequency. We specify the magnitude and phase of $H(e^{j\omega})=A$, we apply (3.47) and carry out the integral to get the signal $h[n]$. The rectangular pulse (3.48) (Fig.3-15a) as an ideal bandlimited signal is a good example of this process, which is a function that is nonzero in the low-frequency band $|\omega| \leq \omega_b$ and zero in the high-frequency band $\omega_b < \omega \leq \pi$. If the nonzero portion of the DTFT is a constant value of A with a phase of zero. [65]

then we have:

$$H(e^{j\omega}) = \begin{cases} 1 & |\omega| \leq \omega_b \\ 0 & \omega_b < |\omega| \leq \pi \end{cases} \quad (3.48)$$

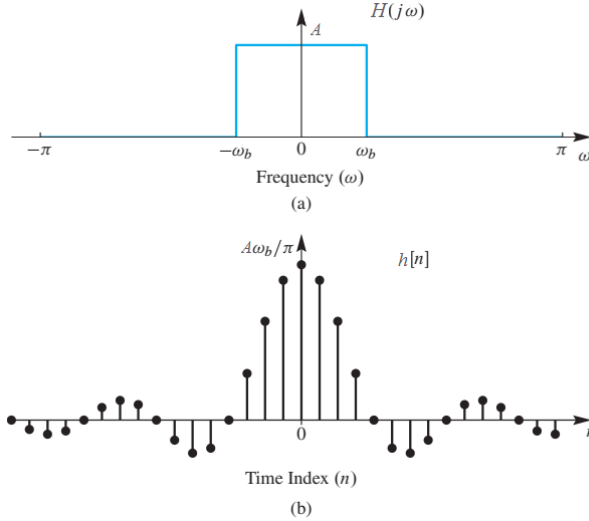


Fig. 3-15. Bandlimited DTFT. (a) DTFT is a rectangle bandlimited
 (b) Inverse DTFT is a sampled sinc function.

This mathematical form, which is called a “sinc function,” is plotted in Fig. (3-15b).

Inverse DTFT:

$$h[n] = \int_{\omega=-\pi}^{\omega=\pi} H(j\omega) \cdot e^{j\omega n} d\omega \quad (3.49)$$

Where $H(j\omega) = A$:

$$h[n] = \int_{-\omega_b}^{\omega_b} H(j\omega) \cdot e^{j\omega n} d\omega \quad (3.50)$$

$$h[n] = \frac{A}{2\pi} \left[\frac{e^{j\omega n}}{jn} \right]_{-\omega_b}^{\omega_b} = \frac{A}{2\pi \cdot jn} [e^{j\omega_b n} - e^{-j\omega_b n}] = \frac{A}{\pi n} \left[\frac{e^{j\omega_b n} - e^{-j\omega_b n}}{2j} \right]$$

$$h[n] = \frac{A}{\pi n} [\sin(\omega_b n)] \rightarrow \frac{A\omega_b}{\pi} \frac{\sin(\omega_b n)}{\omega_b n}$$

$$h[n] = \frac{A\omega_b}{\pi} \text{SINC}(\omega_b n) \quad (3.51)$$

- **Crossing points and amplitude of lobes**

The sinc function (Fig.3-15b) appears to be undefined at $n=0$, application of Hospital’s rule, or the small-angle approximation to the sine function, shows that the value is actually

$$h[0] = A\omega_b/\pi.$$

A key point of the sinc function is the location of the zero crossings. Sinc function cut the zero when $h[n]=0$, it means that the term of $\sin(\omega_b n)=0$ is equal to zero. This condition will satisfy where: $\omega_b n=m\pi$ for each $m \in Z$.

Therefore:
$$n = \frac{m\pi}{\omega_b} \tag{3.52}$$

For $m= \pm 1, \pm 2, \pm 3, \dots$ we have zero-crossing points and n is equal to the number in which sinc function has zero value.

It is seen, the value of the main lobe at $n=0$ can be calculated by $h[0] = A\omega_b/\pi$. If we define the amplitude of bandlimited pulse (rectangular pulse) equal to $A=1$ the main lobe value is dependent on the upper band and lower band value (ω_b) and have $h[0] = \omega_b/\pi$ value or if we desire the sinc function which is main lobe equal to one ($h[0] = 1$) we need to adjust and determine the bandlimited pulse amplitude by calculation value of A .(3.53) If needs $h[0] = 1$ then:

$$A = \pi/\omega_b \tag{3.53}$$

We assume this interval $[-\pi, \pi]$ is divided by $N=10000$ samples, therefore, the interval (2π) is equal to 100000 samples.

$$\pi = \frac{N}{2} = \frac{10000}{2} = 5000$$

And ω_b is corresponds to step frequency, $\omega_b=50$. Therefore:

$$A = \frac{N/2}{\omega_b} = \frac{5000}{50} = 100$$

This value is equal to the amplitude of FFT amplitude which is determined by (3.54):

$$A = \frac{N}{2\omega_b} \tag{3.54}$$

For this study, in the frequency domain, the FFT of the designed sinc the magnitude represents the value of 100 (for normalizing sinc and $(N = 10000)$). The amplitude can be calculated using

$$A = \frac{10000}{2 * 50} = 100$$

In the next subsection, the concept of sinc function designing and relations are expressed.

3.8.3 Sinc calculation

Consider the sinusoidal waveform (fig.3-16) which is sampled by N sample rate, divided in $T_0 = N.T_S$

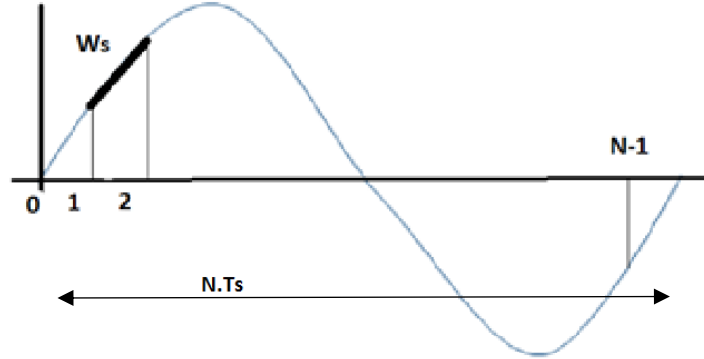


Fig. 3-16

In time domain for the sinusoidal signal can be seen:

$$\sin(\omega t) = \sin(x) \quad (3.56)$$

In continuous form: $\sin(x + T) = \sin(x) \quad (3.57)$

We define period: $T = 2a$

For T period we have ω radian so: $2a = \omega T \rightarrow \frac{2a}{T} = 2a.f \quad (3.58)$

In the discrete form, the length of the curve along each sample is ω_s (3.59).

$$\omega_s = \frac{2a}{N} \quad \omega = k.\omega_s \quad \omega = k.\frac{2a}{N} \quad (3.59)$$

$$f_s = \frac{1}{T_S}, \quad f_0 = \frac{1}{T_0} = \frac{1}{N.T_S} \quad (2.60)$$

f_s is equal to the frequency of sampling in DAQ board (3.26) this frequency may differ and change for other DAQ boards. DAQ board that we use in all tests works to $f_s=500000$ samples per second. We divided the bandlimited (rectangular window signal) as input at the frequency domain and sinc signal as an output in the time domain by $N=10000$. We define f_N :

$$f_N = \frac{1}{N} \quad (3.61)$$

$$f_{0t} = \frac{f_s}{N} \quad (3.62)$$

We must consider in sampling during one second by DAQ board, in which how many cycles of sinc function we have concerning the number sample for each sinc signal. By dividing the

DAQ sample frequency to samples in each sinc signal (3.62) the repetition sequence is funded, this parameter is called f_{0t} which is also equal to step frequency.

$$f_N = \frac{f_{0t}}{f_s} \frac{1}{N} \rightarrow \frac{f_s}{f_{0t}} \quad (3.62)$$

Where: f_s is the sample rate of DAQ board, f_{0t} is repetition frequency and N is the number of samples in sinc function. It means.

As we know FFT of sinc function makes a rectangular signal shape, which contains all frequency components (spectral bound) as is shown in (fig.3-17). The bandwidth of this spectral, determine the minimum and maximum frequencies that must use for designing desire sinc signal. Frequency of signal which is applied to LPVT is f_{0t} in the time domain, this value is equal to step frequency at the frequency domain. It means that if apply FFT on sinc signal in the time domain, it can be seen that the components in the frequency domain just have differences equal to this step frequency. in the other hand, if step frequency has been $f_{0t}=50$, thus, the components in the frequency domain start from 50hz, 100hz, 150hz,.....to maximum component (f_{0x}) which FFT is a non-zero value. The FFT result will be zero after the maximum component (f_{0x}). It should be considered step frequency at frequency domain always is equal to the repetition frequency of the signal in the time domain that is applied to LPVT in other words repetition of sinc signal in one second.

In the frequency domain we can write:

$$f_N = \frac{f_{0x}}{f_s} \rightarrow f_{0x} = f_N \cdot f_s \quad (3.63)$$

Where f_{0x} is a step frequency in the frequency domain.

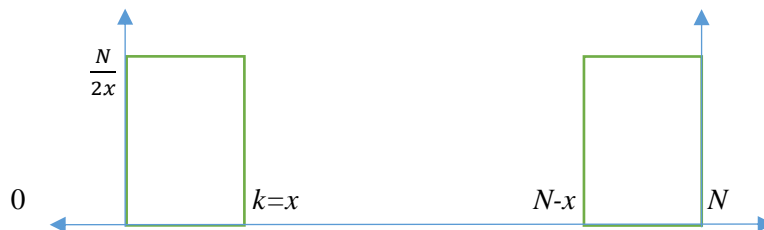


Fig.3-17

As it is seen rectangular pulse in the frequency domain (fig.3-17) contains the frequency components which have differences equal to step intervals or step frequency (f_{0t}). Also (f_{0x}) is the maximum component of the rectangular signal in the frequency domain which FFT results in getting the zero value after this component. The number of these components in each

step frequency in rectangular signal in the frequency domain (according to Fourier transfer) is corresponding to the number of lobes (x) that instructs the sinc signal in the time domain. Therefore, in determining rectangular pulse with specific min and max frequencies, if interval steps frequency increases (f_{ot}), the number of corresponds lobes(x) in sinc signal in time domain decreases because of the number of components in each step to reaching maximum component decreases (3.65).

For clear this subject we refer to (fig.3-16) and (fig.3-167 and by using (3.58) and (3.59)

$$\text{If } k=x: \quad \omega = \frac{2ak}{N} = \frac{2ax}{N} = 2af_N \rightarrow f_N = \frac{x}{N} \quad (3.64)$$

Therefore: by combining two equations (3.58) and (3.59) we have:

$$f_{0x} = \frac{x}{N} \cdot f_S \quad (3.65)$$

In the time domain we have: $f_N = \frac{f_{ot}}{f_S}$ so at the result:

$$f_{0x} = x \cdot f_{ot} \quad (3.66)$$

This last equation (3.66) expresses the relation between frequency steps in the frequency domain and the number of samples in each step and the maximum component in a rectangular signal. to clear the definition of lobes number and step interval frequency the example is expressed.

For instance: If the number of lobes in sinc signal is equal to 50 in the time domain, and $f_{ot}=100$ in the frequency domain, this means that according to step number, for each step until 100 steps, it contains 50 samples for each step, in this way from min to the max component we have 100 steps and 50 samples in each step.

The number of lobes is divided by two series half of them in right and other in the left side of sinc signal, because of the sinc function cross the zero and according to (3.15) and (fig.3-31), sinc signal at integer coefficient of 2π becomes zero value. Moreover, the negative frequency is a meaningless definition. Therefore, for N samples in sinc signal, we have x lobes in which divided into two series on each side of sinc signal. These lobes represent the frequency components in rectangular pulse in the frequency domain which are the FFT of these samples have a nonzero value. According to couple lobes series in two sides in the frequency domain, the rectangular spectral is separated into two parts with nonzero FFT, from 0 to component corresponds to x and from component $(N-x)$ to (N) , for other samples the FFT is zero, this concept is illustrated in (fig.3-17).

In the frequency domain, the components that have nonzero FFT are equal to $2x$ in both upper and lower separate bounds at these two spectral, the amplitude of FFT result for FFT length equal to N is $(N/2x)$. Therefore, by divide the FFT amplitude to N sample, it can be found amplitude for all components which are non-zero FFT value, these are equal to the Fourier coefficients with an amplitude equal to $(1/2x)$. So, we have sinusoidal components with $(1/2x)$ amplitude which is added to gather and finally make the desire sinc signal. For each lobe, it can be possible to calculate the amplitude by using (3.67)

$$\text{lobe amplitude} = \frac{f_{0x}}{(2k + 1)N/2} \quad (3.67)$$

Where k is the number of each lobe.

In this thesis, we need to design the sinc signal for bandlimited signal in the frequency domain by: $f_{0x} = 2500 \text{ Hz}$, by considering sample per second in DAQ board $f_s = 500 \text{ K} \frac{S}{s}$ and sampling points in time domain $N=10000$, x can be calculated by using(2.63):

$$x = \frac{f_{0x} * N}{f_s} = \frac{2500 * 10000}{500000} = 50$$

Then, it can be possible to calculate the frequency steps in the frequency domain, using (3.66)

$$f_{ot} = \frac{f_{0x}}{x} = \frac{2500}{50} = 50$$

As a result, the characteristics of the desire sinc function will obtain $[-50, 50, 10000]$.

Therefore, the sinc function is designed in time domain ranging from -50 to $+50$ passing through 100 integer numbers and 25 lobes on each side.

The FFT amplitude will be:

$$\frac{N}{2x} = \frac{10000}{2 * 50} = 100$$

And coefficient amplitude for Fourier terms is $1/100= 0.01$. These coefficients amplitude apply to Trek amplifier (gain= 20000) to boost the sinc signal to make a sinc signal with an amplitude that we need to apply to LPVT in experimental tests.

- **Signal design considerations**

In this thesis according to the range of power quality frequency range ($0 -2500 \text{ Hz}$), the sinc function which is designed must be in the range from -50 to $+50$ passing through 100 integer

numbers in which the zeroes of sinc function appear. According to the definition of sinc function, the normalized sinc function has one main lobe in $x=0$ and 25 side lobes on each side of the main lobe. The amplitude of each lobe in the sinc function decays as $1/x$. The number of samples is $N = 10000$, for points $N = \pm 100, \pm 200, \pm 300, \dots$ the value of sinc function is zero and we have zero crossings at this points and for points $n = \pm 150, \pm 250, \pm 350, \dots$ we have interval maximum and minimum lobes.

The number of samples ($N=10000$), frequency range (0-2500Hz), also resolution step (50Hz) and being constant the value of $h[0]=1$, impose on the trade-off to determine the number of lobes in each side (25) of sinc function, zero-crossing points (100 points), the amplitude of corresponds lobes and amplitude of bandlimited pulse (rectangular pulse) (100).

The trade-off between the main parameters in designing shows: by reducing the frequency step (f_{0t}) the number of lobes (x) will be increased and sinc amplitude will be decreased, also by increasing the bandwidth value (f_{ox}) the sinc amplitude will be increased. The sinc amplitude in ($n=0$) has inverse proportional to the amplitude of the bandlimited pulse in the frequency domain.

The created sinc signal is regenerated periodically with a step frequency of 50 Hz. The time-domain normalized sinc function designed for the sinc response test is shown in (Fig.3-18)

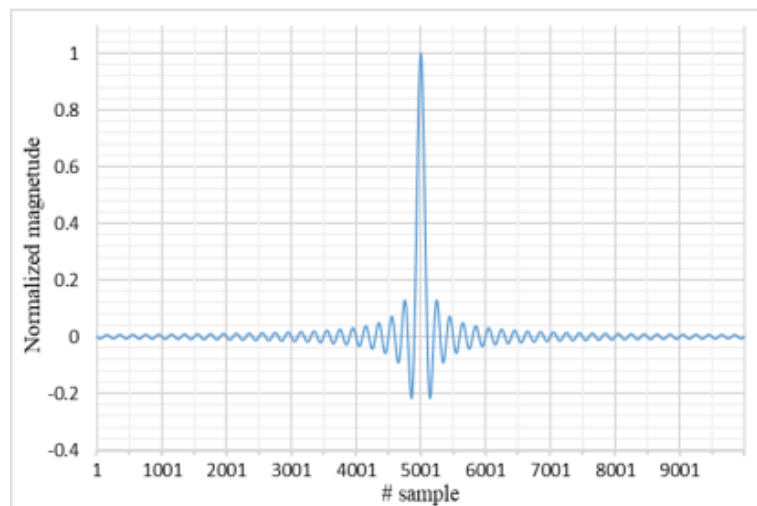


Fig. 3-18

In the next chapter, this method and the experimental test set up will be explained.

In this thesis, a synthesized sinc signal is applied to a capacitive low-power voltage transformer (LPVT) to characterize it in the power quality frequency range. As it is seen, a key feature of

the sinc function is the location of the zero crossings, zeroes of a sinc function appears on integer numbers. Moreover, according to the number of lobes in sinc function and frequency of the sinc function, the width of each lobe is large enough to be sampled and measured with ADC used in Data Acquisition Board (DAQ).

So far, it is explained the procedure and some mathematical points of view to design the sinc function as an impulse signal that we must imply to our dynamic system (LPVT) to attain sinc response and impulse response as well in the range of frequency includes the power quality frequency rang. As we know that the Sweep frequency response test characterizes dynamic systems by applying each frequency separately which is time-consuming because for this reason it is tried to do this test in a one-time test compared to the sweep frequency test which has to be repeated for all desired frequencies. Moreover, the remarkable points to design the proper sinc function which is desired are expressed by relevant examples. In the next chapter, it is going to explain the experimental test and introduce the tools and measurement equipment that we utilize. Practical methods and devices which are involved to measure and computerize the archived data from tests will represent.

3.9 Measured parameters and tests

To characterize the LPVT, several experimental tests setup and procedures are designed. We are facing the voltage sensor that transforms and reduces input voltage to lower voltage at output corresponding to the relative ratio, output voltage components (ratio and phase) follow the input correspond component in ideal LPVT. The ratio represents how output voltage follows the input voltage and phase displacement expresses how the output waveform is similar to the input waveform. Because of presence uncertainty and non-ideal LPVT, these two parameters are changed. The sources of this non-ideally in capacitive LPVTs are the frequency dependency of the primary capacitance dielectric permittivity (resin injection methods and insulation properties) and the resistive leakage of the primary capacitance. These uncertainties express its impact on ratio, phase displacement, and accuracy class. Therefore, output voltage involves errors in ratio and phase displacement which are changed in each LPVT to another one. Thus, we need to define the concept of these errors by determining the ratio error ε and phase displacement error $\Delta\varphi$. Moreover, according to [66], the accuracy performances of an LPVT are expressed by its accuracy class, which defines specific limits for the ratio error ε and the phase error $\Delta\varphi$. The definitions of the above parameters are:

$$\varepsilon = \frac{k_r U_s - U_p}{U_p} \quad (3.68)$$

$$\Delta\varphi = \varphi_s - \varphi_p \quad (3.69)$$

In (3.68), k_r is the rated transformation ratio, U_s and U_p are the RMS values of the actual secondary and primary voltage, respectively, at rated frequency. Also, φ_s and φ_p are the secondary and primary phases, respectively. The relation between voltage phasor of input and output on LPVT can be represented as:

$$\overline{U_p} = \frac{\overline{U_s}}{k_r} (1 + \varepsilon) e^{j\Delta\varphi} \quad (2.68)$$

In this equation, let us denote by $\overline{U_s}$ the phasor of the input voltage U_s , by $\overline{U_p}$ the phasor of the output voltage U_p of the LPVT. Moreover, k_r let be the rated transformation ratio of the LPVT. [67]

By using the LabVIEW program the ratio error and phase displacement error calculate and extract from input and output measured voltages. As we are seen, to assess the LPVT behavior we need to supply the sinc signal to approve this method, the results must be compared with the results of sweep frequency response that is tested by pure sinusoidal waveform. Therefore both test sinc response and sweep frequency response tests are achieved and compared. The absolute ratio errors and phase displacement errors are calculated and compared with reference values which are provided by the standard.

To approve the sinc signal method two different tests have been performed. One is the LPVT characterization by exploiting the presented sinc response approach; another is the well-known sweep frequency response which has been used as a reference method to assess the previous one. The peak voltage for both the sweep frequency response test and the sinc response test is 16.2 kV under the LPVT rated value.

3.9.1 Sinc response test

The purpose is to apply the amplified sinc function to the LPVT, measuring the output, and computing ε and $\Delta\varphi$ for each frequency ranging from 50 Hz to 2.5 kHz with a frequency step of 50 Hz. To perform the test, the sampled designed sinc function saved in a text file is loaded on an Agilent 33250A 80 MHz Function/arbitrary waveform generator. The arbitrary waveform generator output is amplified by the Trek high voltage power amplifier, and then

applied to the LPVT. The applied signal, the sinc function, has a period of 20 ms. Afterward, ε and $\Delta\phi$ at each frequency component have been computed in the LabVIEW software environment acquiring the primary and secondary voltages by NI 9222 DAQ. For the sinc response test, 500 sinc signal with 50 Hz frequency has been applied and for each frequency harmonic, the mean value of 500 measurements is considered. This implies that the test duration is only 10 s.

3.9.2 Sweep frequency response test

The sweep frequency response test aims to compare the results of a consolidated approach to those of the SR test described in the previous subsection. To this purpose, three random frequencies have been chosen as reference: 50 Hz, 500 Hz, and 1 kHz. For each frequency, one sinusoidal signal at the LPVT rated voltage has been generated and applied to it. As in sinc response test, for sweep frequency response test 500 period of sine wave signal with 50 Hz frequency has been applied and for each test frequency, the mean value of 500 measurements is considered. This implies that each frequency test duration is only 10 s. Afterward, ε and $\Delta\phi$ have been computed to be compared with the ones obtained from the SR tests.

3.10 The transfer function of LPVT

The necessity of dynamic modeling and definition of (LPITs) as a system to purpose identification, the definition of features, frequency analysis, and responses are presented. Recognizing the model of LPVT helps to understand how the quantities analysis could be effected on applications and responses of the LPVT model. Moreover, the model of LPVT will be considered and focused. Since the impulse signal has a very short time length and it is not recognizable to detect by data acquisition chain and for measure and computerize measurement values. We have to use a data acquisition board. Moreover, working by data acquisition will be brought us some restrictions because of the limitation on the sample rate. Therefore, to reach a better resolution to detect signal it is better to utilize sinc signal as an impulse signal. Actually, for impulse response analysis, the main considerations are the definition of suitable, valid model and exposition of systems, transfer function, and also impulse signal characteristic.

Such this model is specifically developed to support the analysis, specification, design, verification, and validation of an LPVT as a system. Characterization and modeling of dynamic systems with impulse response test is a well-known procedure. The impulse response test provides dynamic system behavior for all the frequencies at the same time. This procedure is a

one-time test compared to the sweep frequency test which has to be repeated for all desired frequencies

Any linear discrete-time system can be fully described in the time domain by the sinc response $h(t)$. The $h(t)$ describes the response of the system to the infinitely sinc impulse. For an LTI system, the input $X(j\omega)$ and output $Y(j\omega)$ signal in the frequency domain are related via the frequency response $G(j\omega)$ (transfer function) (3.69), which is the FFT of the impulse response

$$F(h(t)) = \frac{F(y(t))}{F(x(t))} = \frac{Y(j\omega)}{X(j\omega)} \quad (3.69)$$

Where : F is the symbol for FFT. Therefore, the output signal in the frequency domain $Y(j\omega)$, and in the time domain $y(t)$, can be calculated as:

$$Y(j\omega) = G(j\omega) \cdot X(j\omega) = F[h(t)] \cdot F[x(t)] \quad (3.70)$$

$$y(t) = F^{-1}[Y(j\omega)] \quad (3.71)$$

Where F^{-1} stands for *IFFT*. This transformation approach for the calculation of the output of a linear system (3.71) is an approach which is explained before. This is one of the main objects in which we can find the correct and proper sinc response (3.70) for describing the LPVT transfer function.

By applying the sinc signal which is designed in the previous section and amplify by TREK and record the output of the experimental setup input (using reference capacitor divider). It can be possible to achieve a sinc response. In the next step, by imply FFT over both signals on both side of LPVT, and extract ratio errors and phase errors and compare the results with the same process without any experimental set, and just using simulation and convolution the sinc signal which is a design by LabVIEW or Matlab, it is capable to approved the sinc response and the $h(t)$ as a representation of LPVT model. Moreover, for validation of the $h(t)$ of LPVT in additional simulation, we apply the harmonic sinusoidal signal with 3rd, 5th, 7th, and combination of 357th harmonics and compare with results by the same harmonics signal which experiments by using setup test. All ratio errors and phase errors from the results of simulations and the experimental test will extract and compare with corresponds simulation and tests. To approve and validate the accuracy of $h(t)$ the ratio error and phase error differences must be lower values which are determined in relevant standards.

CHAPTER 4

EXPERIMENTAL TEST

4 Experimental test

Instrument Transformers (ITs) are conventionally used for monitoring, measuring, and protection purposes. To measure both voltage and current as state variables for power networks, Voltage Transformers (VTs) and Current Transformers (CTs) are deployed. To face the new requirements after the development of the so-called Smart Grids, a new generation of ITs has been developed. These are referred to as Low Power Instrument Transformers (LPITs) or sensors. LPITs in both active and passive configurations are progressively deployed in power networks for their small size, high-frequency bandwidth, and accurate operation for measuring purposes. For these reasons, studies on LPITs are becoming more and more popular in the current literature.

To characterize any dynamic system in whatever range of frequencies, including the Power Quality range, the Impulse Response (sinc response), and the Sweep Frequency Response tests are well-known in the literature. The sinc response test used for characterization at different ranges of frequencies is presented. The sweep frequency response test characterizes dynamic systems by applying each frequency separately. Sweep frequency response test is time-consuming compared to sinc response test as it is a series of consequent tests for each frequency. This chapter is started from the sinc response idea to present a new test signal to test capacitive low-power voltage transformers (LPVTs) in the power quality frequency range (50 Hz – 2.5 kHz). Such a signal, detailed in the last chapter, is a bandlimited pulse (rectangular window pulse) in the frequency domain, which results in a sinc signal in the time domain.

What follows is structured as: describe the sinc function generation setup and introduce some brief explanation of the relevant devices and software program, briefly introduce the LabVIEW software and intuition for the concept of sinc test design. In the next sections, the measurement setup and the experimental tests are described, respectively.

4.1 Setup test

In this thesis, the Sinc Response, in comparison to impulse response, is introduced as an improvement of impulse response test with specified limited range of frequency but with a high resolution detected response.

To implement a test setup to characterize the LPVT, it is must use the sinc function. To generate the sinc signal that we design in the last chapter, it is utilized the Agilent 33250A 80 MHz Function/arbitrary waveform generator (appendix1), GPIB (General Purpose Interface Bus)

interface and LabVIEW program. The sinc signal according to designed parameters and waveform simulates in the LabVIEW program which Agilent 33250A is modulated as several blocks. These blocks are designed by National Instruments that can simulate and provide a suitable data interface to connect the virtual area to real components and measurement devices via the GPIB interface. (Fig.4-1) shows the data flow of the LabVIEW program that is implemented Agilent 33250A to develop sinc signal data points which can be uploaded over GPIB interface to Agilent generator. The five steps of this procedure are listed in the following paragraph.

- **LABVIEW software**

LabVIEW (Laboratory Virtual Instrument Engineering Workbench) software, a product of National Instruments, is a powerful software system that accommodates data acquisition, instrument control, data processing, and data presentation. LabVIEW that can run on PC under Windows, uses graphical programming language (G language), departing from the traditionally high-level languages such as the C language, Basic or Pascal. All LabVIEW graphical programs, called Virtual Instruments or simply VIs, consist of a Front Panel and a Block Diagram. Front Panel contains various controls and indicators while the Block Diagram includes a variety of functions. The functions (icons) are wired inside the Block Diagram where the wires represent the flow of data. The execution of a VI is data-dependent which means that a node inside the Block Diagram will execute only if the data is available at each input terminal of that node. LabVIEW incorporates data acquisition, analysis, and presentation into one system. For acquiring data and controlling instruments, LabVIEW supports IEEE-488 and RS-232 protocols as well as other D/A and A/D and digital I/O interface boards. The Analysis Library offers the user a comprehensive array of resources for signal processing, filtering, statistical analysis, linear algebra operations, and many others. LabVIEW also supports the TCP/IP protocol for exchanging data between the server and the client. LabVIEW v.5 also supports Active X Control allowing the user to control a Web Browser object. [68]

- **GPIB interface**

GPIB (General Purpose Interface Bus) interface has its origin in the HPIB (Hewlett Packard Interface Bus) for interfacing their instruments. GPIB interface is a parallel 24 conductor bus. It includes eight data lines for control messages that are often ASCII encoded, and various management and handshake lines. Handshaking is used to transfer messages between the PC

and the instrument being controlled. GPIB interface and it's a connection to pc-LabVIEW and Agilent 33250A is depicted in (Fig.4-1).



Fig.4-1

4.1.1 Arbitrary Waveform

An overview of the steps required to download and output an arbitrary waveform over the remote interface (GPIB) is expressed in the following. The commands used for arbitrary waveforms are listed.

1 Download the waveform points into volatile memory.

You can download from 1 point (a dc signal) to 65,536 (64K) points per waveform. You can download the points as floating-point values, binary integer values, or decimal integer values. Use the DATA command to download floating-point values from -1.0 to +1.0. DAC command to download binary integer or decimal integer values from -8191 to +8191. To ensure that binary data is downloaded properly, you must select the order in which the bytes are downloaded using the FORM: BORD command.

2 Select the waveform frequency, amplitude, and offset.

Use the APPLY command or the equivalent FREQ, VOLT, and VOLT: OFFS commands to select the frequency, amplitude, and offset of the waveform

3 Copy the arbitrary waveform to non-volatile memory.

You can output the arbitrary waveform directly from volatile memory or you can copy the waveform to non-volatile memory using the DATA: COPY command.

4 Select the arbitrary waveform to output.

You can select one of the five built-in arbitrary waveforms, (in this thesis the sinc signal is selected) one of four user-defined waveforms, or the waveform currently downloaded to volatile memory. Use the FUNC: USER command to select the waveform.

5 Output the selected arbitrary waveform.

Use the FUNC USER command to output the waveform previously selected with the FUNC: USER command.[69]

The data points are saved and can be recalled in the sequence of tests. (Fig.4-2) is depicted as the setup to generate sinc signal and deployed to the main setup test.

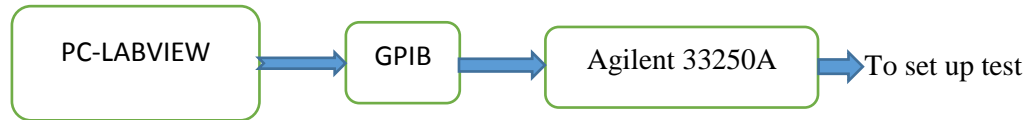


Fig.4-2

According to what we need to sinc response test and the frequency range for the sinc function.it is fixed from 50 Hz to 2.5 kHz which concerns the power quality frequency range in power networks. The sinc function is designed in time domain ranging from -50 to +50 passing through 100 integer numbers in which the zeroes of sinc function appear. According to (1), the normalized sinc function has one main lobe in $x = 0$ and 25 side lobes on each side of the main lobe. The number of samples is $N = 10000$, which is shown in (Fig.3-18). The sinc signal is provided and can apply the LPVT that is seen in (Fig.4-3).



Fig.4-3

- **TREK amplifier**

The sinc signal must have enough energy to impact LPVT and overcome the voltage drops that exist in the setup test. For this purpose, the amplitude of sinc signal is boosted using a High Speed/High Voltage power amplifier. Based on voltage and frequency characteristics which are determined by manufactories the inject voltage should be in nominal voltage range.

In this thesis, Trek speed/high voltage power amplifier model 20/20C-HS is utilized to amplify the generated signal to the 16.3 kV peak rated voltage by 20000 amplitude coefficient, the main characteristics are listed in Table.IV.

Table IV. Trek power amplifier features

Output voltage range	0 to 20 kV DC or AC peak
Input voltage range	0 to 10 V DC or AC peak
DC voltage gain	20000 V/1 V
DC voltage gain accuracy	<0.1 % of full scale
Slew rate	800 V/ μ s
Signal bandwidth	DC to 5.2 kHz
Drift with time	<50 ppm/h
Drift with Temperature	<100 ppm/ $^{\circ}$ C

Trek speed/high voltage power amplifier Model 20/20C-HS is a DC-stable, high-speed, high-voltage power amplifier [70] used in industrial and research applications. It features an all-solid-state design for a high slew rate, wide bandwidth, and low noise operation. The four-quadrant, active output stage sinks or sources current into reactive or resistive loads throughout the output voltage range. This type of output is essential to achieve an accurate output response and a high slew rate demanded by a variety of loads such as highly capacitive or reactive loads. It is configured as a non-inverting amplifier.

Schematics of the Trek amplifier are shown in (Fig.4-4).



Fig.4-4

4.1.2 Data Acquisition Chain

A data acquisition chain typically consists of several parts such as:

Sensors, which measure physical variables (temperature, strain, pressure, flow, force and voltage, and current).

Signal conditioning, to convert the sensor output into signal readable by the analog input board (A/D) in the PC.

An analog input (A/D) board, to convert these signals into a digital format usable by the PC.

A computer software, with the appropriate application software to process, analysis and log the data to risk. (Fig.4-5) is illustrated the concept of the data acquisition chain.

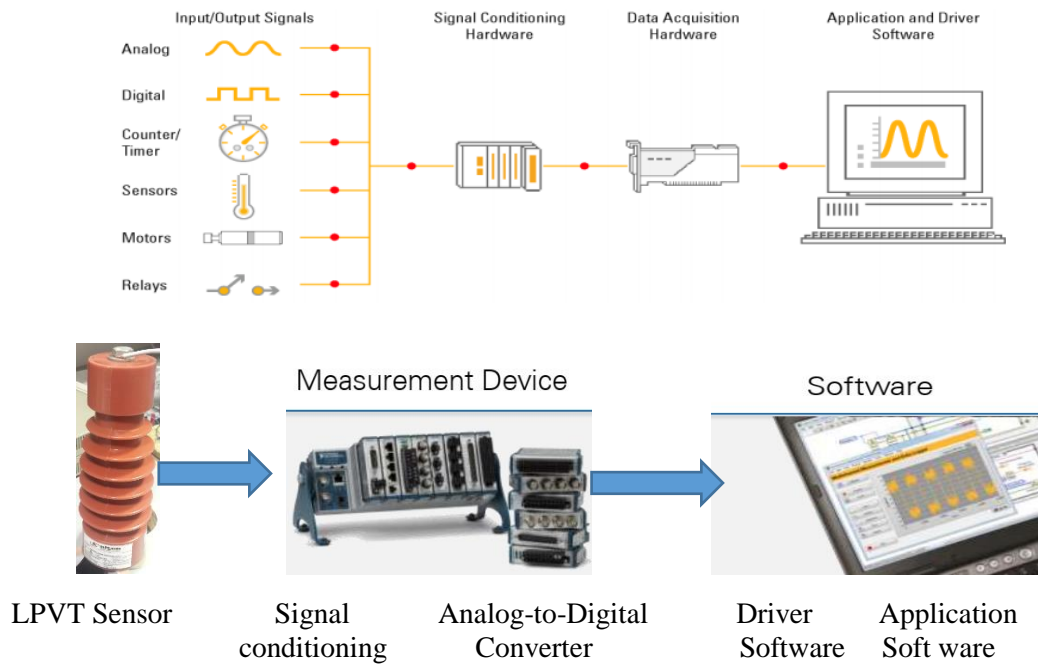


Fig.4-5.data acquisition chain

NI Compact DAQ hardware combines a 1, 4, or 8-slot chassis with over 50 measurement-specific NI C Series I/O modules and can operate stand-alone with a built-in controller or connect to a host computer over USB, Ethernet, or 802.11 Wi-Fi. All National Instruments data acquisition (DAQ) devices are packaged with NI-DAQ driver software. [71]

- **DAQ consideration**

After installing LabVIEW and the NI-DAQ driver, LabVIEW uses the software configuration information to recognize your hardware and to set default DAQ parameters. When you launch the program, NI-DAQ displays a list of all of the devices on your computer. You can edit the default settings for parameters, such as analog input polarity and range on a per-device basis and you can configure channels. It can be given each channel configuration a unique name that is used when addressing your channels in LabVIEW. The DAQ address many common applications involving data acquisition in LabVIEW. You can find the Data Acquisition VIs in the Functions palette from your block diagram in LabVIEW. Most of the DAQ VI subpalettes arrange the VIs at different levels according to their functionality. The Easy VIs usually are composed of Intermediate VIs, which are in turn composed of Advanced VIs. Also, it can be possible to use Intermediate Vis, utility, and advanced Vis. The device input on the analog I/O, digital I/O, and counter VIs specifies the number the DAQ configuration software assigned to your DAQ device. The Analog Input VIs have a channel list parameter, where you can specify the channels from which the VIs read or write, If we use the DAQ Channel Wizard to configure

analog and digital channels, we can address our channels by name in the channel list parameter in LabVIEW. By using Limit settings are the maximum and minimum values of the analog signal(s) we are measuring or generating if it acquires data from more than one channel multiple times, the data is returned as a two-dimensional (2D) array. But in this thesis, we use the (1D) array. [72], [73]

Now that we have defined the signal, you must choose a measurement system. We have an analog signal, so it must convert the signal with an ADC measurement system, which converts the signal into information the computer can understand. Before choosing a measurement system we must determine ADC bit resolution, device range, and signal range. It can be compared to the resolution on a DAQ device to sample per second criteria. The more sample rate that we have, the more precise in measurements. The higher the resolution, the higher the number of divisions into the system can break down the ADC input level range, and therefore, the smaller the detectable change. The input level range refers to the minimum and maximum analog signal levels that the ADC can digitize. The smallest detectable in this thesis is corresponds to the smallest lobe in sinc function which must detectable by DAQ board. Because the main problem in capacitive LPVT characterization with impulse response test is the short pulse width of impulse response and technical limitations for detecting such short width signal. This limitation is imposed by a limited range of sampling frequency for Analog to Digital Converters (ADC). The resolution of the measured IR signal should be high enough to detect the slight frequency dependency of a capacitive LPVT, but the frequency dependency of LPVT is very small since they are quasi-ideal sensors. The sources of non-ideally in capacitive LPVTs are the frequency dependency of the primary capacitance dielectric permittivity and the resistive leakage of the primary capacitance. Moreover, we should consider the signal limit setting in which, a more precise limit setting allows the ADC to use more digital divisions to represent the signal.

4.2 Measurement setup

The test setup implemented to characterize the LPVT is depicted in (Fig.4-6) and (Fig.4-7), the test setup is composed of:

- Agilent 33250A 80 MHz Function/arbitrary waveform generator used to generate the designed sinc signal.

- Trek High Speed/High Voltage power amplifier Model 20/20C-HS to amplify the generated signal to the 16.3 kV peak rated voltage. Its main characteristics are listed in Table IV.
- Passive capacitive LPVT under test with $\frac{20}{\sqrt{3}} kV/\frac{2.73}{\sqrt{3}} V$ rated voltage and 0.5 accuracy class.
- Resistive-capacitive reference voltage divider with $\frac{20}{\sqrt{3}} kV/\frac{3.34}{\sqrt{3}} V$ rated voltage and 0.1 accuracy class to measure the primary signal and used it as a reference.
- NI 9222 Data Acquisition Board with $\pm 10 V$ range and 500 kS/s sampling frequency. Its accuracy features are $\pm 0.02 \%$ gain error and $\pm 0.01 \%$ offset error.

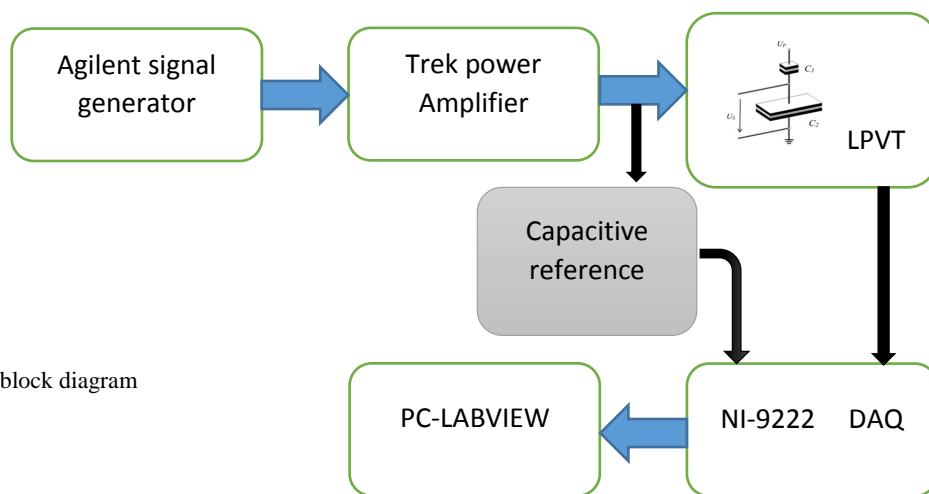


Fig.4-6.setup block diagram

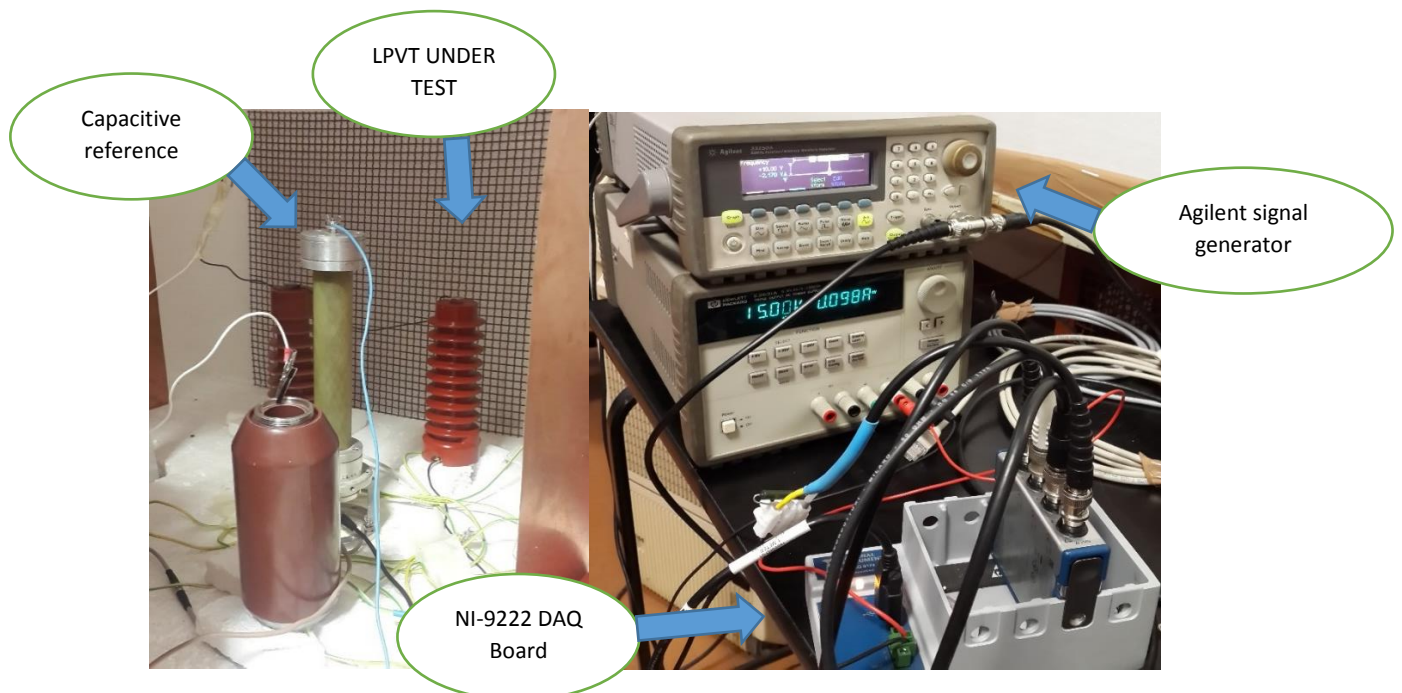


Fig.4-7 setup pictures(LPVT under test install in the electromagnetic chamber)

The required signals are generated and amplified before applying to the LPVT under test. Then, the primary and secondary voltages are acquired to compute ratio error ε and phase displacement $\Delta\varphi$ at each frequency of interest. In brief, Comparing the single frequency test results with the ones from sinc response test, it can be confirmed the effectiveness of this method. In fact, as confirmation by the absolute variation values, all ε and $\Delta\varphi$ values lies within 10 %. Therefore, the results show that it is possible to confirm the effectiveness of the proposed sinc response test. Firstly it is a one-time test compared to the time-consuming SFR test. Secondly, the accuracy obtained with the sinc response test is aligned and compared with one of the sweep frequency response tests. In the next chapter, the results are expressed by details.

All ratio error and phase displacement errors of input and output of LPVT are collected and saved in text file corresponds to each sample point. In particular, the ε and $\Delta\varphi$ values at a period of frequencies 50, 500, and 1000 Hz have been extracted from the sinc response test results to determine $H(s)$ which is represented as an impulse response.

4.3 Approval and validation tests

In the previous sub-section, the procedure of sweep frequency response (sinusoidal waveform) and sinc response test and experimental test setup was explained. The results of these tests will describe in the next chapter. These two tests are shown the sinc response test is almost the same results in comparison to sweeping frequency response in an acceptable error range. Also, it is shown this method (sinc response) can be accepted as a better and more effective way for frequency response analysis in a one-time test instead of separated frequency tests. But for studying and reaching the dynamic model of LPVT and determine the acceptance model which represents the dynamic behavior of LPVT as a function $h(t)$. It is necessary to do more experimental tests. Determining the $h(t)$ response to achieve the behavior of LPVT when imposes to sinusoidal harmonics signal and sinc signal in different voltages can reveal the more features and characters of LPVT.

4.3.1 Sinc response test in different voltages validation

By using experimental setup in (Fig.4-6), LPVT is tested by sinc signal in different voltages (20kv, 16.2kv, 12.2kv, 8.1kv, 4kv) to understand the behavior of LPVT to different voltage levels. Moreover. All results are computerized and recorded as ratio error and phase error in text format for 10000 sample points. For each voltage step, sinc signal at the input of LPVT is sensed by the reference capacitor divider. Results of FFT in both signals measured and absolute

value (norm of FFT) and phases separately by software and the ratio and phase error for both measured values are calculated and archived in a text file. The $h(t)$ is represented the LPVT transfer function in the time domain which is express the behavior of LPVT. To approval this test we apply the regenerated sinc signal by software and repeat the procedure of measurement and record via simulation. All ratio and phase errors for all sample points are recorded, the results of simulations and experimental tests are compared based on standard acceptable values to approve results or reject.

4.3.2 Harmonic tests validation

The LPVT is tested by impure sinusoidal that add the different harmonics (3^{th} , 5^{th} , 7^{th} and the combination of these three harmonics, 3^{rd} , 5^{th} , 7^{th}) to validate the accuracy of $h(t)$ also to clarify the LPVT behavior response to almost real and actual conditions in networks and field. As the test sequences are explained in the previous paragraph, contaminated sinusoidal signal to several harmonics is applied to LPVT. The output of reference capacitance divider and output of LPVT measured and the results of FFT are recorded and norm and phase for both sides are extracted. All values archived as a text file. By software program, the ratio and phase error is extracted. On the other hand, the harmonics signal is regenerated by software and impose to $h(t)$ and after implying to FFT the norm and phase calculate and ratio errors and ratio and phase errors are extracted and compared to other results. Finally, these two achievements compared with standard to validation.

In the next chapter, the results of sinc response method and results of sinc tests in different voltages and also results of the contaminated sinusoidal signal by harmonics and other results will be expressed.

CHAPTER 5

RESULTS

5 Results

The experimental results are reported in this chapter, the sweep frequency response results are compared with the result from sinc response test to approve this new method, and also the results are commented and discussed. In the last but not least chapter, briefly summarizes the achievements and the conclusion and some prepositions will be expressed.

The results of sinc response experimental tests on different voltages (20kv, 16.2kv, 12.2kv, 8.1kv, 4kv) and results of the simulation the sinusoidal harmonic for harmonics (3rd, 5th, 7th) and a combination of these three harmonics, 3rd, 5th, 7th to validate the $h(t)$ are express in this chapter.

5.1 Results of a new method of sinc response

Two different tests have been performed. One is the LPVT characterization by finding the presented sinc response approach, another is the well-known sweep frequency response which has been used as a reference method to assess the previous one. The peak voltage for both the sweep frequency test and sinc response test is 16.2 kV following the LPVT rated value.

5.1.1 SR test results

The ratio error (ε) and phase error ($\Delta\varphi$) results of the sinc response tests are collected in (Fig.5-1) and (Fig.5.2), respectively. Before detailing them, it is worth to recall that the tested LPVT has an accuracy class of 0.5 which corresponds to maximum limits for ε and $\Delta\varphi$ of $\pm 0.5\%$ and ± 6 mrad, respectively. In (Fig.5-1) it is shown that the ratio error increases from first to third harmonic and then decreases as the frequency increases. (Fig.5-2) shows phase displacement computed for all harmonics and an extreme decrease can be seen from first harmonic to a few harmonic orders.

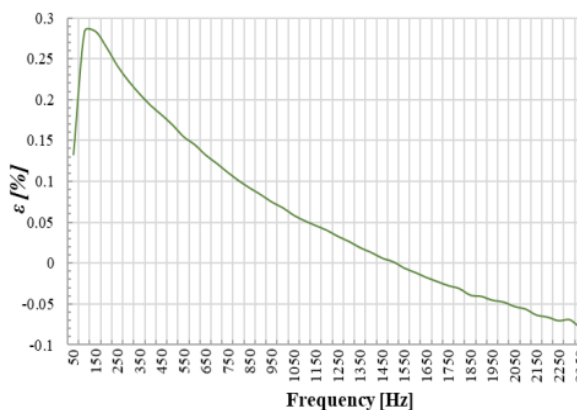


Fig. (5-1) Ratio Error trend vs. frequency

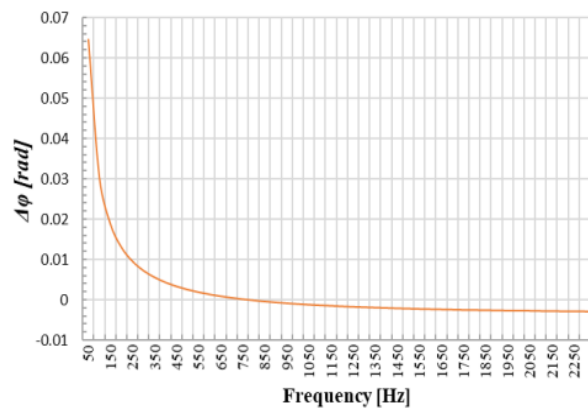


Fig. (5-2)Phase Displacement trend vs. frequency

At 50 Hz, ε and $\Delta\varphi$ are 0.13 % and 0.0646 radians. The ratio error is correctly within the limits of the LPVT accuracy class; as for $\Delta\varphi$ instead, it is out of limits because no correction factor has been applied. Capacitive LPVT fabrication suffers from an accurate design of primary capacitance in terms of persistence transformation ratio and phase displacement from one sensor to another. Normally this problem is solved with two solutions: one, providing the customer with unique correction factors for both ratio and phase displacement, and second, by compensating the error by internal active electronics to place the ratio and phase displacement in the range declared in nameplate which makes the LPVT an active LPVT. The LPVT used in this work is a passive sensor.

5.1.2 Sweep frequency test results and comparison

To verify the sinc response test results with a single frequency test, in (table V) all ε and $\Delta\varphi$ have been collected. In particular, the ε and $\Delta\varphi$ values at frequencies F 50, 500, and 100 Hz have been extracted from the SR test results. Besides, the table shows the absolute variation of both ε and $\Delta\varphi$ between the two cases, ε and $\Delta\varphi$, Respectively. Comparing the single frequency test results with the ones from sinc response test, it can be confirmed the effectiveness of the latter method. As confirmed by the absolute variation values, all ε and $\Delta\varphi$ values lie within 10%.

Table V. Sinc response test and sweep frequency response test results

F [Hz]	SFR		SR		Absolute Variation	
	ε [%]	$\Delta\varphi$ [rad]	ε [%]	$\Delta\varphi$ [rad]	$\frac{\varepsilon}{\varepsilon}$ [%]	$\frac{\Delta\varphi}{\Delta\varphi}$ [%]
50	0.1435	0.064691	0.13	0.0646	9.41	0.15
500	0.1638	0.002444	0.17	0.0024	3.79	1.80
1000	0.0761	-0.001190	0.07	-0.0011	8.02	7.56

(Table V) reports the mean values of 500 measurements for both sinc response and sweep frequency response tests. Considering the standard deviation for each measurement, the number of significant digits represents the order of relevant uncertainty. As it was predictable, the uncertainty associated with the sinc response results is 2 orders of magnitude greater than those of the sweep frequency response results. The single sinc signal used for the sinc response test has a limited resolution for testing all frequencies from 50 Hz to 2500 Hz. On the contrary, during the sweep frequency response tests, it is possible to adjust the sine wave to the desired resolution in a more accurate way. However, the obtained uncertainty is sufficiently low to

assess the computed quantities ε and $\Delta\phi$. Therefore, in light of the results in (Table. V), it is possible to confirm the effectiveness of the proposed sinc response test.

In conclusion, in this thesis, the sinc signal is applied to a capacitive LPVT to characterize it in the power quality frequency range. Then, the obtained results are compared, in terms of ratio error and phase displacement with the typical sweep frequency test performed on the transformer. From the comparison, it is possible to confirm the applicability and accuracy of the developed characterization procedure. Therefore, the sinc response can be used to fast characterize the transformers, so that it is a “one-time” test compared to the time-consuming sweep frequency response test and the accuracy obtained with the sinc response test is aligned and compared with the one of sweep frequency response test.

5.2 $h(t)$ transfer function

The main propose of this thesis is to identify and achieving the transfer function that can capable to characterize and reveal the behavior of LPVTs so that by utilizing this function it can be possible to express all responses to any input signals. According to the control system concepts and definition about the transfer function, the quotient of the division of output signal to the input signal in the frequency domain and apply the IFFT to result of this division, the function of the system in the time domain is attained. On the other hand, the results of sinc response test are approved that applying sinc signal to a capacitive LPVT to characterize it in the power quality frequency range. By comparing results with sweep frequency response, it could be possible to confirm the applicability and accuracy of the developed characterization procedure. Therefore, the sinc response can be used to fast characterize the transformers.

TABLE.VI .recorded parameters from the experimental test (20kv,sinc signal) in excel program

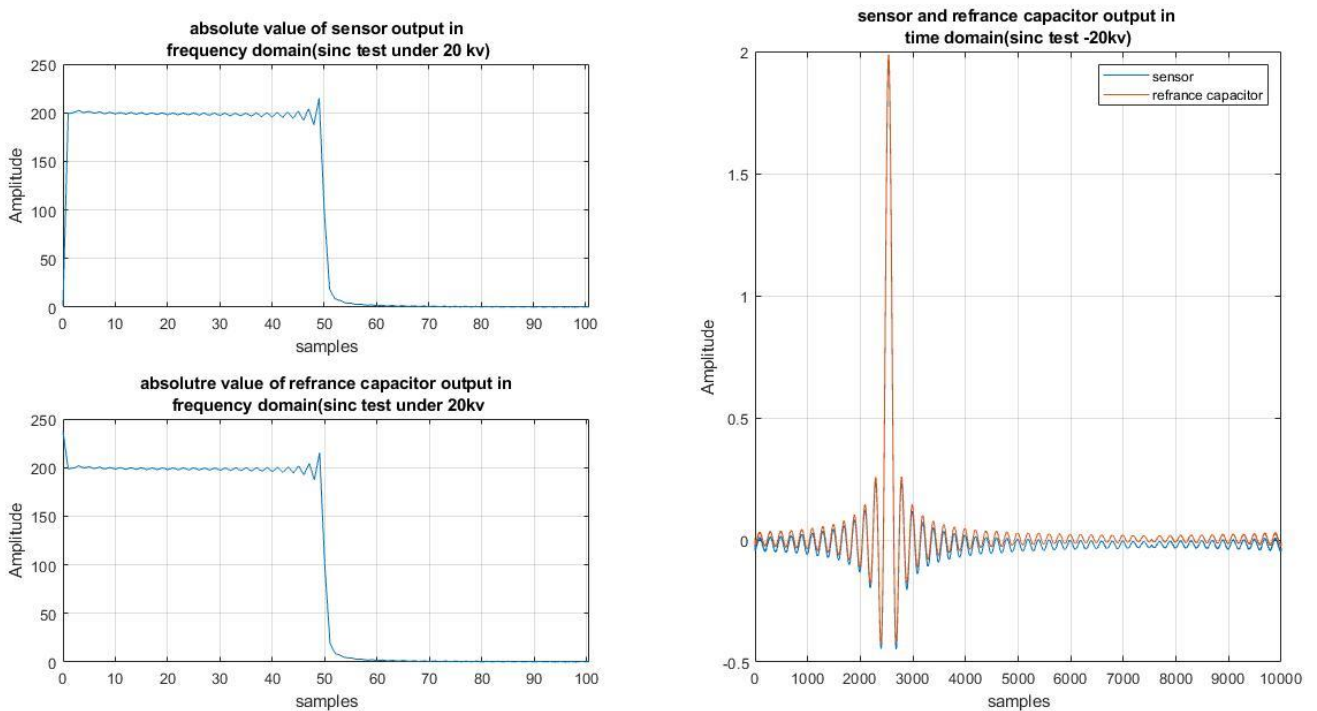
frequency component	abs. value sensor output	std. abs. value sensor output	phase sensor output	std. phase sensor output	radius ref.C.D. output	std. abs. ref. C.D. output	phase ref.C.D. output	std pahse ref.C.D. output
0	1.674493253	0.364547309		0	237.1702583	0.152849998	0	0
1	199.016025	0.720464742	-1.529557825	0.000721801	198.7219208	0.716666995	-1.596640132	0.000715729
2	200.1203853	0.039531563	3.132767065	0.002156895	199.5337358	0.039846338	3.100062903	0.002157706
3	202.2719334	1.053127888	1.523130264	0.005424363	201.7095753	1.051577663	1.501974124	0.005431529
4	200.1438225	0.027680302	-0.083198239	0.004331859	199.6218644	0.025591095	-0.098588648	0.004333812
5	201.3718394	0.228988205	-1.682294437	0.005851299	200.8771813	0.229655312	-1.694187563	0.005853526
:	:	:	:	:	:	:	:	:
:	:	:	:	:	:	:	:	:
9999	200.1203853	0.039531563	-3.132767065	0.002156895	199.5337358	0.039846338	-3.100062903	0.002157706
10000	199.016025	0.720464742	1.529557825	0.000721801	198.7219208	0.716666995	1.596640132	0.000715729

In sinc response test to explore $h(t)$, the absolute value and phase displacement of reference capacitor divider is selected from experimental test results as the input signal of LPVT and also absolute value and its phase displacement of the sensor(LPVT) are chosen as an output signal

in the frequency domain,(Table.VI), then, the 10000 numbers of samples change to complex numbers to keep the features of these two signals, based the definition of the transfer function (3.69), for all samples points(10000), the value of $H(S)$ are calculated in Matlab program which is written for this purpose. All results are changed to the time domain by applying IFFT and at the end, $h(t)$ of LPVT is achieved.

To approval the $h(t)$, in this stage the same sinc signal which is achieved from the output of reference capacitor and transferred to time domain is applied to $h(t)$ using coevolution, but in this stage convolving the sinc signal with $h(t)$ and all procedure are given by Matlab program.

(Fig.5-3a) is depicted the similarity of the absolute value of output results which are derived



from

(a)

(b)

Fig5-3. Comparison between the sensor and reference capacitor output in the frequency domain(left-figure a) and comparison between sensor and reference capacitor divider output in the time domain(right-figure-b)

experimental test over sensor under test and applied sinc signal to $h(t)$ which is calculated by the convolution via Matlab program.

According to the sinc signal which is designed in chapter 3, with this features[-50, 50, 10000], the interval step frequency is 50Hz, as it is seen the cut-off frequency is exactly 50Hz in the frequency domain, by considering the numbers of lobes (50) in sinc signal, the maximum frequency which FFT has value will be 2500 Hz.

(Fig.5-3a) and are shown the one part of window spectral [0 to 50] another part of the window is [9950-10000]. Moreover, it is seen in (Fig.5-3a-up) the first component has zero value in the sensor response because the LPVT sensor contains capacitors and in the first component LPVT is applied by DC voltage and has not response against DC voltage but because of the existing resistor in reference capacitor divider in first DC component, the response can be sensitive.(Fig.5-3a-down). As it is explained in the last paragraph the cut off frequency exactly matches in 50 Hz.

(Fig.4-3-b) is illustrated the comparison between output sinc signal applied to sensor and reference capacitor in the time domain which is achieved using IFFT of output signals directly. This figure shows the impact of ratio differences and also phase displacement differences which are explained in sweep frequency test and sinc responds test in the last subsection.

5.3 Approving $h(t)$ accuracy

It is seen by using control system theory and signal system relation, the model of LPVT is introduced. Applying sinc signal to LPVT and record data in the input signal and output of LPVT helped to achieve $h(t)$ of LPVT which is represented this model and identified the behavior of the LPVT model. For approving this model, the data which are derived from the experimental test setup must compare to data that is achieved from the simulation. And the final result to approval the accuracy of the defined LPVT model must be in the range of values that determined in the relevant standards.

5.3.1 Result test under different voltage and frequencies

In this subsection, the resulting test under different voltages and frequencies is expressed. To survey the LPVT response under different voltages and different sinc signal frequencies we apply a different range of voltages(16.2kv, 12.2 kV, 8.1kv, 4kv) to apply LPVT and repeat the test in different frequencies (50 Hz, 500 Hz, 1 kHz, 1.5 kHz, and 2.5 kHz). The results can be shown in (table.VII) and (fig.5-4) and (fig.5-5).

For different scenarios the ratio error (ϵ [%]) and phase displacement error ($\Delta\phi$ [rad]) are calculated and recorded in (table.VII). It can be noted, because of the limitation of the capability of the TREK amplifier to supply the enough current to set up in higher frequency and additionally impedance reduction corresponding to total capacitance effect in set-up test, the result for frequencies 1.5kHz, 2.5kHz in 16.2kv and 12.2kv are not able to measure. Moreover, for the same reasons tests for 20kv are not possible and results are not recorded.

Table.VII.compare the results of simulation and test result in the ratio error and phase displacement error in different frequencies and different voltages

frequency	Voltage test	16.2kv		12.2kv		8.1kv		4kv	
	Type of results	ε [%]	$\Delta\varphi$ [rad]	ε [%]	$\Delta\varphi$ [rad]	ε [%]	$\Delta\varphi$ [rad]	ε [%]	$\Delta\varphi$ [rad]
50 Hz	Exprimental test	0.14333	0.06469	0.14307	0.06470	0.14331	0.6463	0.14178	0.06461
	Simulation	0.1428	0.0671	0.1417	0.0670	0.1550	0.0671	0.1451	0.0668
500 Hz	Exprimental test	0.16559	0.00244	0.16983	0.00239	0.16108	0.00239	0.16064	0.00238
	Simulation	0.16451	0.00268	0.1670	0.00219	0.1654	0.0029	0.1676	0.0026
1 kHz	Exprimental test	0.07617	-0.00119	0.06876	-0.00118	0.06885	-0.00118	0.06990	-0.00118
	Simulation	0.0776	0.0013	0.0663	0.0013	0.0672	0.0013	0.0660	0.0013
1.5 kHz	Exprimental test	0	0	0.03123	-0.00233	0.03055	-0.00233	0.03172	-0.00231
	Simulation	0.0322	-0.0733	0.0319	-0.0028	0.0316	-0.0026	0.0320	-0.0019
2.5 kHz	Exprimental test	0	0	0	0	-0.00618	-0.00309	-0.00692	-0.00312
	Simulation	-0.0894	-0.0062	-0.0310	-0.0064	-0.0073	-0.00551	-0.0077	-0.00350

It is considered that increasing frequency has a low variation on the ratio error ε [%], and fell to negative values but by decreasing applied voltage, the ratio error ε [%] variation has some fluctuation around the same value for each frequency. phase displacement error $\Delta\varphi$ almost is constant in each frequency and for constant voltage by increasing frequency fell to negative values .the all values in experimental test and simulation are less the values which determine in standard (less than 10%), it is worth to recall that the tested LPVT has an accuracy class of 0.5 which corresponds to maximum limits for ε and $\Delta\varphi$ of ± 0.5 % and ± 6 mrad, respectively. and the result of experimental tests and values which are achieved from simulation approve the accuracy in acceptable range according to the standard. The ratio error is correctly within the limits of the LPVT accuracy class; as for $\Delta\varphi$ instead, it is out of limits because no correction factor has been applied. Capacitive LPVT fabrication suffers from the accurate design of primary capacitance in terms of persistence transformation ratio and phase displacement from one sensor to another.

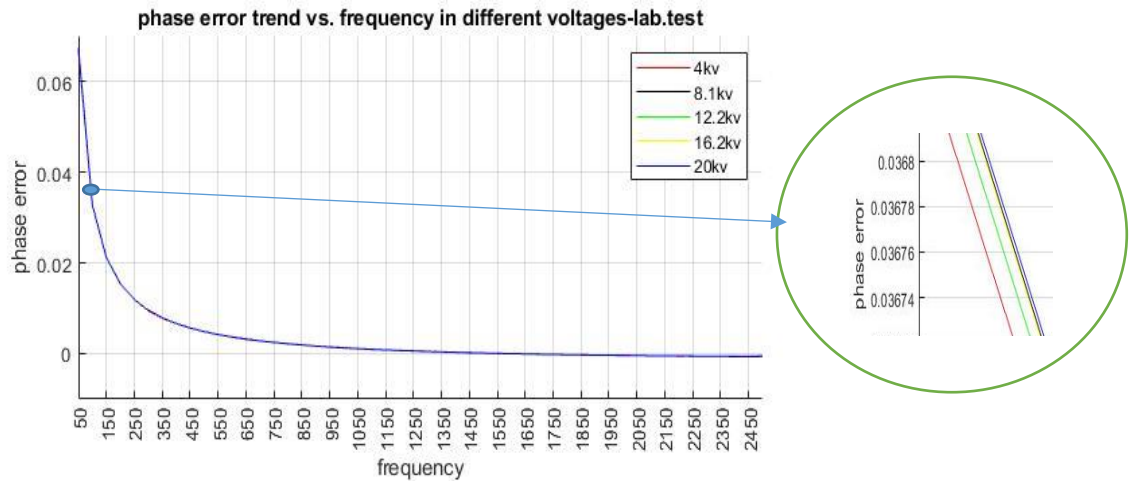


Fig.5-4. Phase displacement trend vs. frequency in different voltages

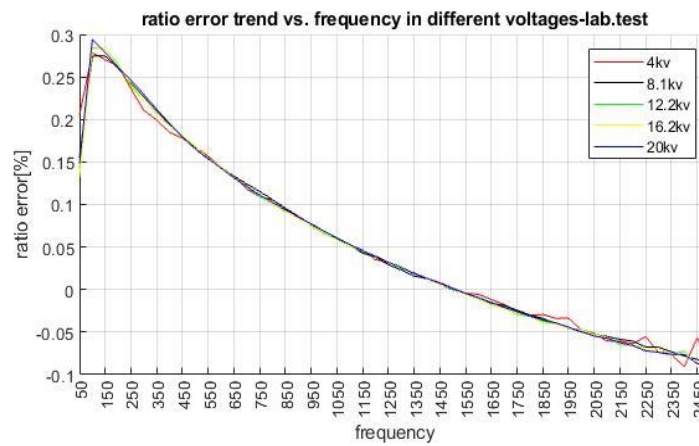


Fig.5-5. Ratio error trend vs. frequency in different voltages

It can be recommended two solutions for this problem, the first, providing the customer with unique correction factors for both ratio and phase displacement, and the second, by compensating the error by internal active electronics to place the ratio and phase displacement in the range declared in name-plate which makes the passive LPVT to active LPVT.

5.4 Results of harmonics test and validation of $h(t)$

So far, it is approved the LPVT $h(t)$ by comparing the ratio error and phase displacement error which are derived from experimental test and simulation program in different voltages for different applied frequency sinc signals. For approval $h(t)$, it must be used the same sinusoidal input signal that contaminated by different harmonics. Simulation results are compared with experimental test results and final results are checked with the standard.

5.4.1 Sinusoidal harmonic results

The new generation of LPVTs is used in medium voltage grids and many industries. In these fields, voltage and current are contaminated by harmonics due to the presence of electronics converters that contain switching circuits and other harmonic resources. The approval, the harmonic test procedure is designed by applying harmonics sinusoidal waveform to achieve the results of the response behavior of LPVT that imposing these signals. For all scenarios, the ratio errors and phase displacement errors are calculated by the simulation program and recorded in the table.VIII.

Table.VIII is illustrated the results for 3rd,5th,7th , and signal that is a combination of these three harmonics (3rd-5th-7th), (Fig.5-6) for each harmonic the valid values belong to fundamental component and one's harmonic. Other components among 10000 frequency components have zero value. Moreover, harmonics combination (3rd -5th -7th) contains a fundamental component and other harmonics which have value among the rest of the samples.

Ratio errors and phase displacements in Simulation results are compared by the experimental test for approving the $h(t)$ transfer function of LPVT and all results are compared to standard values.

Table.VIII. compare the results of simulation and test result in the ratio error and phase displacement error
indifferent harmonics

Number of harmonics	Type of results	ε [%]	$\Delta\varphi$ [rad]	ε [%]	$\Delta\varphi$ [rad]	ε [%]	$\Delta\varphi$ [rad]	ε [%]	$\Delta\varphi$ [rad]
3rd	Experimental test	0.1871	0.0672	0.3093	0.0210	-	-	-	-
	Simulation	0.1478	0.0647	0.2780	0.0187	-	-	-	-
5 th	Experimental test	0.1793	0.0671	-	-	0.2685	0.0119	-	-
	Simulation	0.1478	0.0647	-	-	0.2456	0.0095	-	-
7 th	Experimental test	0.1803	0.0671	-	-	-	-	0.2322	0.0079
	simulation	0.1478	0.0647	-	-	-	-	0.2117	0.0055
3 rd ,5 th ,7 th combination	Experimental test	0.1808	0.0671	0.3073	0.0210	0.2684	0.0119	0.2297	0.0079
	simulation	0.1478	0.0647	0.2780	0.0187	0.2456	0.0095	0.2117	0.0055

Table.VIII is illustrated that an increasing number of harmonics causes very lightly decrement on phase displacement errors in comparison to fundamental frequency, also it can be seen the same variation for ratio error.

It should be considered that the tested LPVT has an accuracy class of 0.5 which corresponds to maximum limits for ε and $\Delta\varphi$ of $\pm 0.5\%$ and ± 6 mrad, respectively. The results of experimental test and values which are achieved from simulation approve the accuracy in acceptable range according to the standard.

For fundamental frequency which is a pure sinusoidal waveform, the results for the experimental test is, $\varepsilon [\%]=0.1871$ and displacement error is $\Delta\varphi[\text{rad}] = 0.0671$. The ratio error is correctly within the limits of the LPVT accuracy class, but for $\Delta\varphi$, it is out of limits because no correction factor has been applied. Moreover, simulation results in fundamental frequency for ratio error is $\varepsilon [\%]=0.1478$ and for displacement error is $\Delta\varphi[\text{rad}] = 0.0647$, it is seen for simulation correspond to $h(t)$ all characterization of LPVT impact on simulation result even no applying correction factor and LPVT ratio and TREK amplifier.

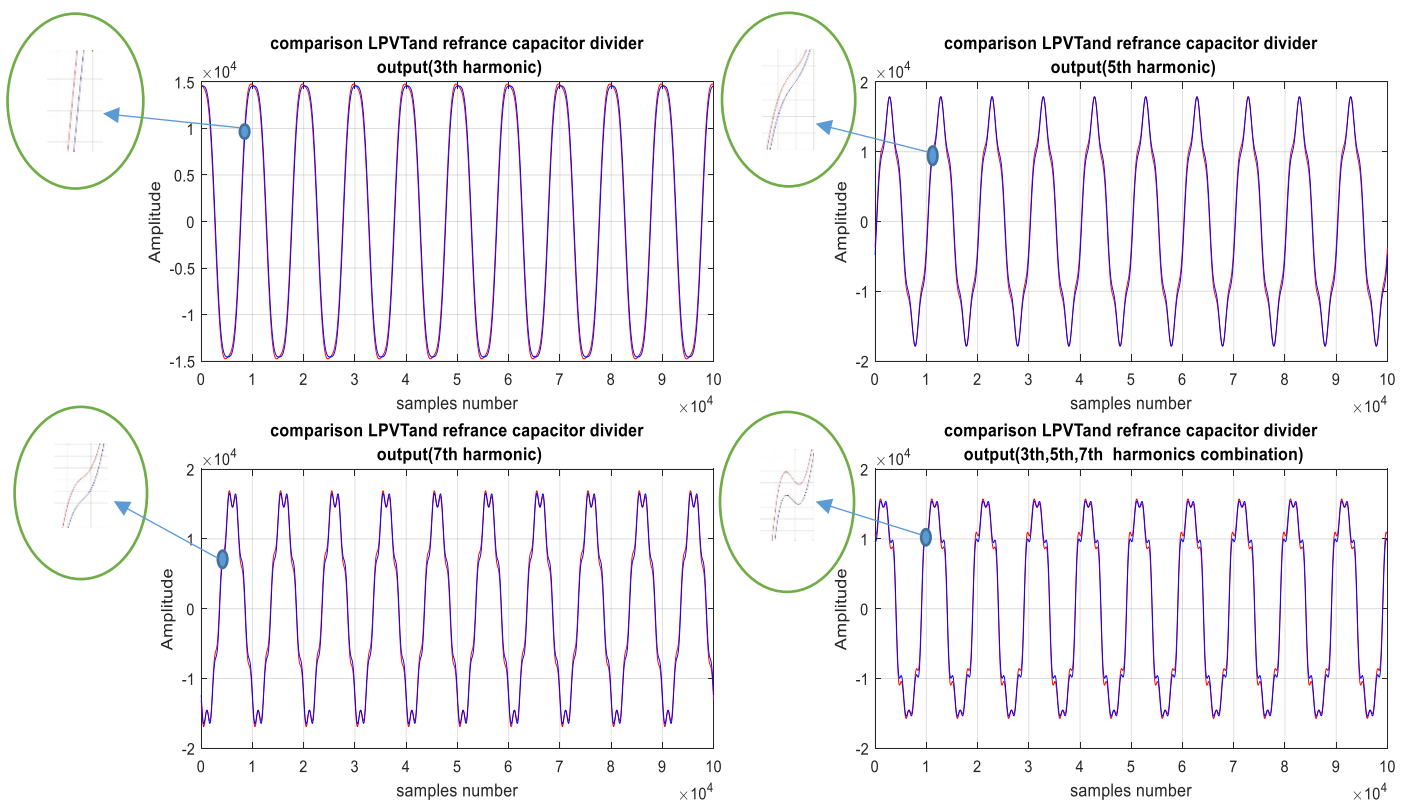


Fig.5-6, comparison of LPVT and refrance capacitor output in different sinusoidal harmonics

The simulation shows the level of amplitude of harmonics can change the distortion and quality of signal waveform, but because of transfer function $h(t)$ of LPVT, ratio errors and phase displacement errors are not changing considerably and accuracy class remains in an acceptable range.

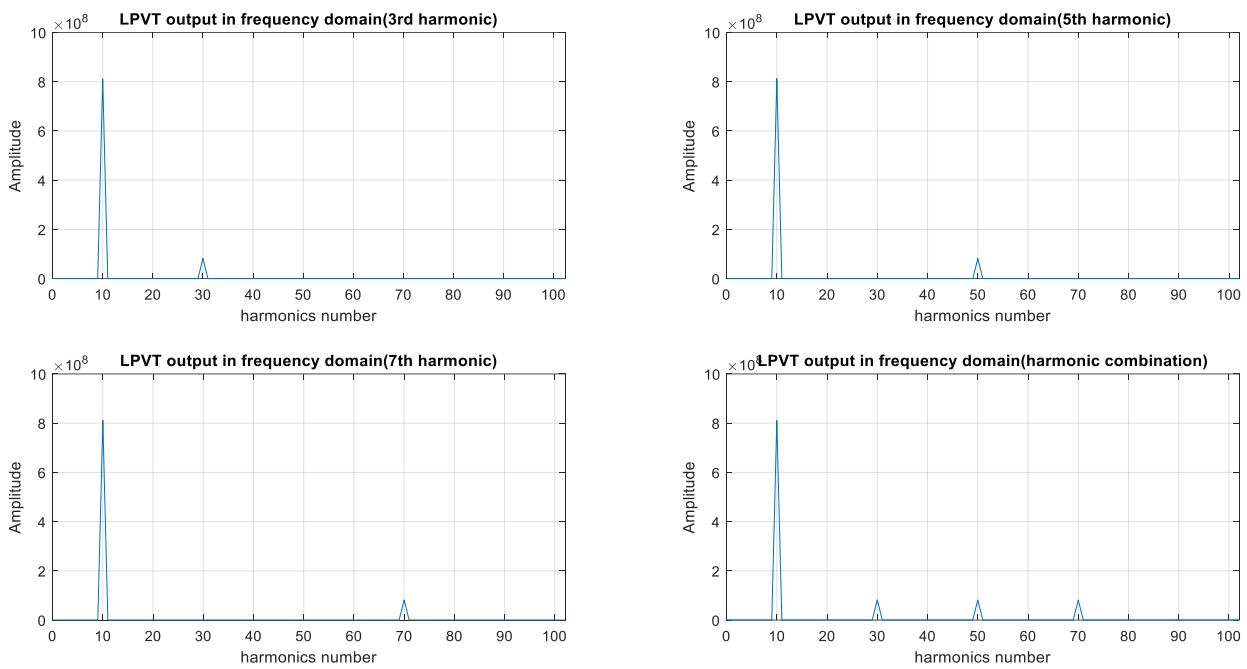


Fig.5-7, LPVT output in different sinusoidal harmonics in the frequency domain

For better understanding, the concept of approval similarity of experimental test trend and output of LPVT in the frequency domain are depicted in (Fig. 5-7) according to the value of harmonic contamination the amplitude of harmonic component can be changed at frequency trend, in this thesis, the amplitude of 3rd harmonic, 5th harmonic and 7th harmonics are considered 0.1 of the fundamental frequency. A combination of three harmonics trends also is shown in (fig.5-7).

5.5 Validation of $h(t)$

A comparison between experimental test result and simulation results to the same input harmonic signal can be ensured that the achieved $h(t)$ contains all characterization of LPVT as a transfer function. Therefore, utilizing the $h(t)$ instead of LPVT in every simulation, designing, and electrical analysis can be independent of every physical presence of LPVT.

The most considerable achievement of this thesis is introducing the new method to attain the model of LPVT as a transfer function which contains all electrical characterizations and behavior of LPVT as a data text file. This data file ($h(t)$ of LPVT) can be used in every test and simulation even other experimental test setups by using a very simple program based on signal and system.

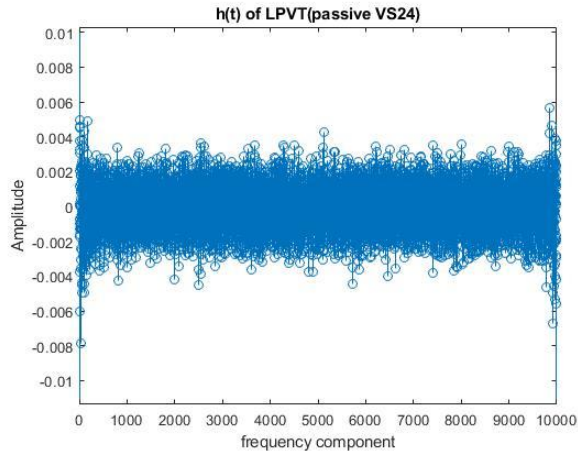


Fig.5-8.data of $h(t)$ of LPVT transfer function vs. 10000 frequency samples for 20kv

To validation of the $h(t)$ of LPVT, there are applied four types of a sinusoidal harmonic signal which is similar to signals that LPVTs have been imposed in real conditions and different electrical fields. All these signals are generated by simulation program and applied and convolved by $h(t)$ and the result of coevolution can be seen in (fig.5-9) for 3rd harmonic, 5th and 7th harmonics, also the result of simulation for the combination of these harmonics and convolution by $h(t)$ is shown in (fig.5-9).

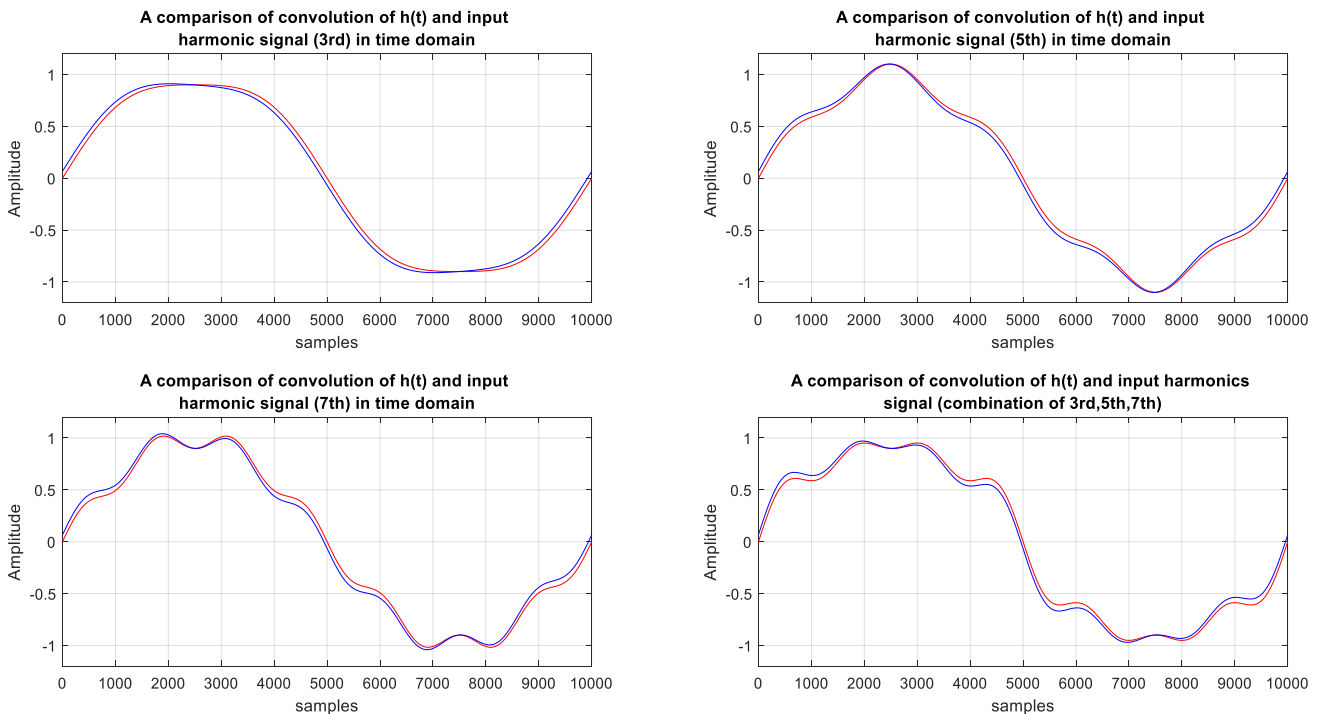


Fig.5-9.convolution result between LPVT, $h(t)$ and sinusoidal harmonic signal contaminated by 3rd,5th,7th and harmonics combination

It must be noted that through the validation procedure, it is just utilities $h(t)$ function which is represented of the LPVT characteristics, and sinusoidal harmonics designed as input corresponds to different scenarios.

For validation, the ratio error and phase displacement error for each scenario is calculated and compared with standard values, Table.IX. is illustrated the results.

Table.IX. compare results of simulation result the ratio error and phase displacement error in different harmonics

Type of results	ε [%]	$\Delta\varphi$ [rad]	ε [%]	$\Delta\varphi$ [rad]	ε [%]	$\Delta\varphi$ [rad]	ε [%]	$\Delta\varphi$ [rad]
3th harmonic simulation	0.1478	0.0647	0.2780	0.0187	-	-	-	-
5 th harmonic simulation	0.1478	0.0647	-	-	0.2456	0.0095	-	-
7 th harmonic simulation	0.1478	0.0647	-	-	-	-	0.2117	0.0055
3rd,5th,7th combination	0.1478	0.0647	0.2780	0.0187	0.2456	0.0095	0.2117	0.0055

Table.IX. is illustrated the simulation results of sinusoidal applied signal to $h(t)$ which are contaminated by different harmonics. Results of convolution these inputs with $h(t)$ are affected in ratio error and phase displacement. It is better to recall that the accuracy characteristics and other electrical features of LPVT transfer to results via $h(t)$ by convolution operation. But the consideration to the maximum limit of accuracy class of LPVT for ratio error (ε [%]=0.5), and also the limitation of phase displacement ($\Delta\varphi = \pm 0.5$ % and ± 6 mrad) can be used as reference criteria to the evaluation of simulation results.

Table.IX. shows that an increasing number of harmonics causes very lightly decrement on phase displacement in comparison to fundamental frequency, and also ratio error decreases as well.

6 Conclusion

This thesis is tried to introduce the new generation of LPVT. The model of LPVT as a transfer function is introduced too, also the application of Sinc signal as an impulse signal is expressed. Moreover, the method of designing Sinc signal according to window pulse is introduced. The LPVT transfer function according to the experimental results is achieved. The transfer function of LPVT data according to frequency components is recorded. The achieved result from the experimental test for sweep frequency response and sinc response are compared and the accuracy of the method is approved. The sinc response test for sinusoidal plus different harmonics is compared with simulation and results are approved the method and accuracy of LPVT transfer function, $h(t)$. Accuracy of LPVT transfer function ($h(t)$) is validated by comparing the result of simulation with the standard. By using this method and extract the $h(t)$ will be one of the important parameters that can be enhanced relevant standard and $h(t)$ can be an imminent characteristic that can be introduced by the producer in the datasheet to use for simulation, design the electrical circuits and research.

REFERENCES

- [1].Roman Malaric. “Instrumentation and measurement in electrical engineering”.2011- Brown Walker Press.
- [2].Alan S. Morris, Reza Langari “Measurement and Instrumentation Theory and Application”, Second Edition, 2016, 2012 Elsevier Inc.
- [3]. Elizete Maria Lourenco ; Antonio Simoes Costa ; Raimundo Ribeiro P., Jr, “Steady-State Solution for Power Networks Modeled at Bus Section Level”, December 2009
- [4]. Wikipedia, the free encyclopedia, “Systems modeling/Types of systems modeling /Systems architecture”, Springer, 2005
- [5]. Paluri Suraj and Patluri Sandeep, “A Study of Impulse Response System Identification”, Karlstad University, lecture note, 2014
- [6]. X-Engineer Organization, Graduate Engineering, “Basic principles of system modeling”, 2019 (<https://x-engineer.org>)

- [7]. Piya Kovintavewat, “Modeling the Impulse Response of an Office Room”, Chalmers University of Technology Goteborg, Sweden, 1988
- [8]. Yan Yinghui, Chen Ming, Cheng Yangchun, “A Nanosecond High Voltage Impulse Protector for small signal measurement device”, International Conference on Intelligent Systems Design and Engineering Application, 2012
- [9]. Yi Q. Sun, Jie Zhang, Tao Cheng, Ning He. “Using Impulse with Appropriate Repetition Frequency in IFRA Test to Diagnosis Winding Deformation in Transformer”, State Grid of Chongqing, Chongqing 401123, 2016 China
- [10]. J. J. Wu, J. J. Huang, T. Qian, W. H. Tang “Study on Nanosecond Impulse Frequency Response for Detecting Transformer Winding Deformation Based on Morlet Wavelet Transform”, international conference on power system technology, November 2018
- [11]. Martin Dadić, Tomislav Župan, Gabrijel Kolar “Finite-ImpulseResponse Modeling of Voltage Instrument Transformers Applicable for Fast Front Transients Simulations”, Journal of Energy, volume 67, 2018
- [12]. IEC 61869-1, Instrument transformers – Part 1: “Additional requirements for low-power passive voltage transformers”, December 2017
- [13]. Pablo Gómez, Francisco de León, Iván A. Hernández, “impulse-Response Analysis of Toroidal Core Distribution Transformers for Dielectric Design”, IEEE Transactions On Power Delivery, vol. 26, no. 2, April 2011
- [14]. R. Lamedica, M. Pompili, B. A. Cauzillo, S. Sangiovanni, L. Calcara, A. Ruvio, “Instrument Voltage Transformer Time-Response to Fast Impulse”, Astronautics, Electrical and Energetic Engineering Department (DIAEE) Sapienza University of Roma, 2016 Italy
- [15]. Theodore S. Rappaport, Scott Y. Seidel, and Kichiro Takamizawa, “Statistical Channel Impulse Response Models for Factory and Open Plan Building Radio Communication System Design”, IEEE transactions on communications, vol. 39, no. 5, May 1991
- [16]. R.K.R. Yarlagadda, “Analog and Digital Signals and Systems”, Springer Science Business Media, LLC 2010
- [17]. Mathew K. Samimi, Theodore S. “Local Multipath Model Parameters for Generating 5G Millimeter-Wave 3GPP-like Channel Impulse Response”, NYU Tandon School of Engineering
- [18]. Jay Anderson – Omicron Academy, “Current Transformer Theory & Testing”, Hands-On Relay School, 2016

- [19]. Electrical Notes & Articles/ “Current transformers Principle of operation of CT”, (<https://electricalnotes.wordpress.com/>) April 16, 2011
- [20]. Digital Energy, “Instrument Transformer Basic Technical Information and Application”, (www.GEDigitalEnergy.com) GE Digital Energy – ITI 1907 Calumet Street Clearwater, Florida, USA, 33765
- [21]. Bin Chen , Lin Du , Kun Liu, “Measurement Error Estimation for Capacitive Voltage Transformer by Insulation Parameters”, 13 March 2017
- [22]. Circuit Globe, electronic instrumentation terms “Transformer Potential Transformer, transform in load conditions”, (<https://circuitglobe.com/potential-transformer-pt.html>)
- [23]. Circuit Globe, electronic instrumentation terms “Transformer Potential Transformer (PT)”, (<https://circuitglobe.com/potential-transformer-pt.html>)
- [24]. RITZ company, RITZ Instrument Transformers GmbH, “Medium Voltage Instrument Transformers”, 01.08.2007, (www.ritz-international.com)
- [25]. Ruthard Minkner Trench Switzerland AG, “Low Power Voltage and Current Transducers for Protecting and Measuring Medium and High Voltage Systems”, 26th Annual Western Protective Relay Conference, October 1999
- [26]. RITZ company, RITZ Instrument Transformers GmbH, “Instrument Transformers /Voltage Transformer”, RITZ Mess wandler Hamburg, 01.08.2007, (www.ritz-international.com)
- [27]. Schneider Electric Industries, “Control and Monitoring/ Only one LPCT for all protection chains based on the circuit breaker and Sepam”, (www.schneider-electric.com)
- [28]. Ager Larrabeiti, Zigor Ojinaga, “Low-power instrument transformer-based MV automation: lessons learned and future applications” 24th International Conference & Exhibition on Electricity Distribution (CIRED) 12-15 June 2017
- [29]. Alessandro Mingotti, Lorenzo Peretto, Roberto Tinarelli, “Low Power Voltage Transformer Accuracy Class Effects on the Residual Voltage Measurement”, IEEE Instrumentation and Measurement Society, 2018
- [30]. IEC 61869-10:2017, Instrument transformers - Part 10: “Additional requirements for low-power passive current transformers”, 2017
- [31]. IEC 61869-11:2017, Instrument transformers - Part 11: “Additional requirements for low power passive voltage transformers”, 2017

- [32]. Rob Kopmeiners, Denny Harmsen, Jens Weichold, “accurate revenue metering with low power current and voltage sensors according to recent IEC 61869-10 and IEC 61869-11 standards”, 25th International Conference on Electricity Distribution Madrid, 3-6 June 2019
- [33]. RITZ company, RITZ Instrument Transformers GmbH, “Instrument Transformers/ Current Transformer”, RITZ Mess wandler Hamburg, 01.08.2007, (www.ritz-international.com)
- [34]. IEC 60044-8:2002, 7th Edition, Instrument transformers – Part 8: “Electronic current transformers”, 2002
- [35]. Schneider Electric Industries, “LPCT technology is the technical answer to the evolution of relay technology that is now based on digital design”, (www.schneider-electric.com)
- [36]. Ritz Instrument Transformers GMBH, “The low-power passive voltage transformer”, Aguste, 2018, (www.ritz-international.com)
- [37]. Ritz Instrument Transformers GMBH, “Medium Voltage Instrument Transformers/ Voltage Transformer Single Pole”, Rev_2014-01, (info@ritz-international.com)
- [38]. IEC-60044:2002, Instrument transformers – Part 1: “Current transformers”, 2001-2002
- [39]. Ritz Instrument Transformers GMBH, “The electronic voltage transformer /DC and AC voltage divider with buffer amplifier”, Aguste, 2018, (info@ritz-international.com)
- [40]. Prysmian Group, “Separable elbow connector Medium Voltage (MV)Up to 12,7/22 (24) Kv, FMCE 25”, (infocables.fr@prysmiangroup.com, www.prysmiangroup.com)
- [41]. Elasco Group, “ MV Separable straight connector for polymeric cable, dead-break operation MSCS/EC”, (<https://www.powerandcables.com>)
- [42]. lumen learning, Physics II, “Capacitors and Dielectrics/ Describe the action of a capacitor and define capacitance”, (<https://courses.lumenlearning.com>).
- [43]. Electronics-Tutorials, “Introduction to Capacitors”, (<https://www.electronics-tutorial.ws>).
- [44]. Electronics-Notes, “Capacitor ESR, Dissipation Factor, Loss Tangent & Q”, (<https://www.electronics-notes.com>)
- [45]. Electronics-Notes, “Dissipation factor and loss tangent definitions, Capacitor Q”, (<https://www.electronics-notes.com>)
- [46]. Griffiths, David J; “Frequency Dependence of Electric Permittivity”, Introduction to Electrodynamics, 3rd Edition 2007

- [47]. Anupinder Singh, Ratnamala Chatterjee, “Origin of Large Dielectric Constant with Large Remnant Polarization and Evidence of Mango - isoelectric Coupling”, Solid State Physics Division, Bhabha Atomic Research Centre, Trombay, Mumbai-400085, India
- [48]. Physics Stack Exchange question and answer site for active researchers, “Real and imaginary parts of dielectric constant”, (<https://physics.stackexchange.com>)
- [49]. Mike Lanagan, “Dielectric Properties and Metamaterials”, Penn State University, January 15, 2008, Kyoto Japan
- [50]. Lennart Ljung, “System Identification Theory for the User”, Second Edition Linkoping University Sweden, 1999
- [51]. Hwei P. Hsu, Ph.D. “Theory and Problems of Signals and Systems”, Schaum's Outlines series, The McGraw-Hill Companies, Inc,1995
- [52]. R.K. Rao Yarlagadda, “Analog and Digital Signals and Systems”, Springer New York,2010
- [53]. Stanley Chan, “Class Note for Signals and Systems”, University of California, San Diego, August 2011
- [54]. Paluri Suraj and Patluri Sandeep, “A Study of Impulse Response System Identification”, Karlstads Universitet, 2014
- [55]. Prof. Paul Cuff, Slides courtesy of John Pauly, “Time Domain Analysis of Continuous-Time Systems, ELE 301: Signals and Systems”, Princeton University, Fall 2011-12
- [56]. Zdenek Matyas and Martti Aro, “HV Impulse Measuring Systems Analysis and Qualification by Estimation of Measurement Errors via FFT, Convolution, and IFFT”, IEEE Transactions on Instrumentation and Measurement · November 2005
- [57]. Dawar Awan, “Analysis of LTI systems (Impulse response, convolution)”, CECOS College of Engineering and IT, March – July 2012
- [58]. R. Kulkarni, “Introduction to Electrical Signals and Systems”, Chapter 4, Frequency Domain and Fourier Transforms” 2001, 2002
- [59]. IEC 61869-6:2016. Instrument Transformers-Part 6: “Additional General Requirements for Low-Power Instrument Transformer”, International Standardization Organization: Geneva, Switzerland, 2016

- [60]. IEC 61000-2006. Standards On Power Quality Part3-Part4: “Emission limits in the frequency range 2 to 9 kHz (in preparation), Test for immunity to conducted, common mode disturbances in the frequency range 0 Hz to 150 kHz”, 2006
- [61]. Dalibor Filipovic- Grčića, “Frequency response and harmonic distortion testing of inductive voltage transformer used for power quality measurements”, 4th International Colloquium, Transformer Research, and Asset Management,2017
- [62]. MIT Open CourseWare, “The Function sinc(x) - Single Variable Calculus”, Fall 2010, (<http://ocw.mit.edu/terms>)
- [63]. Cooper Union, Digital Signal Processing Lecture Notes, “Sinc Functions and Sampling Theory”, October 7, 2011
- [64].R.K. Rao Yarlagadda, “Analog and Digital Signals and Systems”, Springer New York, 2010
- [65]. Georgia Institute of Technology (GT), lecture note “Fourier Transform for Discrete-Time Signals”, Fall2014, (<https://www.coursehero.com>)
- [66]. IEC 61869-13 Instrument Transformers—Part 13: “Stand Alone Merging Unit”, document IEC 61869-13, International Standardization Organization, Geneva, Switzerland, 2018.
- [67]. Alessandro Mingotti, Lorenzo Peretto, Roberto Tinarelli, “Simplified Approach to Evaluate the Combined Uncertainty in Measurement Instruments for Power Systems”, September 2017
- [68].National Instrument-Engineering teaching, “LabVIEW is a development software”, (<https://www.ni.com>), 2019
- [69].User's Guide, “Agilent 33220A-20 MHz Function /Arbitrary Waveform Generator”, chapter 4, 234, (www.Manualslib.com), March 1, 2012
- [70].User's Guide, “Trek Model 20/20C-HS-High-Speed High-Voltage Power Amplifier”, (www.trekinc.com, Trek-CA@aei.com), 2013
- [71].National Instrument-Engineering teaching, “Data Acquisition Practical Session/ Measuring Analog Input Signals” (<https://www.ni.com>), 2019
- [72].Prof. Dr. Tuna Balkan, Lecture Note, Data Acquisition Chain, (<http://www.slideshare.com>), fall 2003-2004
- [73]. National Instrument-Engineering teaching, “Data Acquisition Basics Manual”, January 2000 Edition

